Microglia promote neurodegeneration and hyperkatifeia during withdrawal and prolonged abstinence from chronic binge alcohol

Elizabeth McNair[1,2], Lamar Dawkins[1,2], Grace Ross[2], Alexandra Barnett[1,2], Puja Nakala[2], Liya Qin[2], Jian Zou[2], Viktoriya Nikolova[3,4], Sheryl Moy[3,4], Leon G. Coleman, Jr.[1,2]*

[1]University of North Carolina at Chapel Hill School of Medicine, Department of Pharmacology, Chapel Hill, NC

[2]Bowles Center for Alcohol Studies, University of North Carolina at Chapel Hill School of Medicine, Chapel Hill, NC

[3]University of North Carolina at Chapel Hill School of Medicine, Department of Psychiatry, Chapel Hill, NC

[4]University of North Carolina at Chapel Hill, Carolina Institute for Developmental Disabilities, Chapel Hill, NC

*** Corresponding author:** Leon G. Coleman Jr, 104 Manning Drive, CB7178, Chapel Hill, NC 27599,

leon_coleman@med.unc.edu, Phone: 1-919-966-0501

Abstract

Proinflammatory microglial activation and hyperkatifeia during withdrawal are key features or Alcohol Use Disorder (AUD) as well as in rodent models of binge alcohol. However, it is unclear the role microglia play in the development of AUD behavioral phenotypes, particularly negative affect or hyperkatifeia. We hypothesized proinflammatory microglia promote neuronal death and hyperkatifeia during withdrawal and prolonged abstinence. METHODS: Inflammatory and affective responses were measured in adult mice 24h or 4 weeks after 4 or 10 daily binge ethanol exposures (5g/kg/d, i.g.). RT-PCR was used to measure expression of pro-inflammatory genes. FosB immunohistochemistry was measured in stress circuitry central amygdala (CeA), BNST, and infralimbic cortex (IL) as a proxy for neuronal activity. Behavioral testing was performed in additional cohorts to measure anxiety-like behavior (center time in the open field), hyperarousal (acoustic startle), and inflexible negative affect (conditioned fear memory with extinction). To determine the role of proinflammatory microglia, Gi DREADDs were activated in microglia (CX3CR1.CreERT2.hm4di+/-EtOH +/- CNO). RESULTS: Binge ethanol increased pro-inflammatory gene activation both 24h after EtOH and lasting weeks into withdrawal (type I IFNs). Ten ethanol binges increased FosB in stress circuitry during withdrawal while simultaneously reducing BDNF persistently in the dBNST and CeA. Ethanol-treated mice spent less time in the center of the open field (anxiety-like behavior), had increased magnitude of acoustic startle reflex (hyperarousal) during withdrawal with reduced extinction of conditioned fear memory (PTSD phenotype) 4-5 weeks into abstinence. Gi-DREADD inhibition of microglia during alcohol treatment blocked persistent increases in proinflammatory cytokines, prevented ethanol-induced neuronal death (TUNEL), and prevented ethanol-induced hyperkatifeia including anxiety-like behavior and persistent conditioned fear memory. CONCLUSION: These data find a causative role for microglia in the development of negative affect behaviors during alcohol withdrawal. The prevention of these pro-inflammatory effects and behaviors by microglial inhibition reveals the integral role microglia play in the acute and lasting effects of ethanol on behavior in AUD pathogenesis.

Introduction

Nearly 95 million individuals suffer from Alcohol Use Disorder (AUD) worldwide[1]. AUD is characterized by difficulty in ceasing alcohol use despite adverse effects on health and/or social life[2]. Current treatments for AUD include pharmacotherapies (naltrexone, acamprosate, and disulfiram), behavioral therapies, and support groups[3, 4]. Despite these options, ~60% of individuals with AUD relapse within the first year after treatment[5, 6]. Various health and social factors contribute to relapse, with stress or negative affect states, also known as hyperkatifeia, emerging as a driving force[7-10]. Negative affect states may contribute to increased craving during withdrawal or abstinence to promote relapse[11, 12]. Alcohol misuse is also often co-morbid with mood and affective disorders such as depression and PTSD[13-15]. However, no current therapies for AUD target this alcohol-induced negative affective or hyperkatifeia state. Therefore, the severity of AUD, the difficulty of treating relapses, and the association of AUD with mood disorders warrants a better understanding of alcohol-induced hyperkatifeia.

The natural history of AUD involves earlier stressful life experiences followed by the initiation of binge drinking episodes[16-19]. These experiences interact with more proximal stressors to produce alcohol-seeking behavior[20], with repeated cycles of binge alcohol use and withdrawal promoting hyperkatifeia[21]. Therefore, treatment strategies that interrupt this cycle may be effective at reducing relapse or preventing AUD-related psychiatric disorders. Several studies have focused on neuronal activity in key brain regions and circuits associated with alcohol-related hyperkatifeia and anxiety-like behavior, such as the bed nucleus of the stria terminalis (BNST), central amygdala (CeA), and infralimbic cortex (IL). The BNST has been tied to aversive states and dysphoria during drug withdrawal[22-24], as well as conditioned and unconditioned anxiety responses[25]. The CeA plays a role in the formation of anxiety-like behaviors with alcohol dependence, including fear memory acquisition and extinction[26, 27]. Additionally, the IL is involved in stress-responses and subsequent alcohol-seeking behavior[28, 29]. While much work has been done regarding the role of neurotransmission in these regions as it relates to hyperkatifeia, relatively little is known regarding the role of glia and proinflammatory signaling.

Proinflammatory signaling is a pertinent regulator of neurotransmission, particularly in disease states. Glia, such as microglia and astrocytes regulate neuronal firing, memory, and survival[30-32]. We and others have reported previously that binge ethanol induces proinflammatory polarization of microglia[33-35]. This involves the activation of innate immune pathways, such as NF-kB and resulting expression of pro-inflammatory cytokines (i.e., TNFα, IL-1β, etc)[36]. Correlations between proinflammatory gene expression and lifetime consumption of alcohol in postmortem human AUD brain suggest proinflammatory signaling is heightened with increased exposures[37-40], however, this has yet to be determined experimentally. AUD proinflammatory stimuli, such as toll-like receptor agonists promote alcohol drinking in rodents[41, 42], and microglial depletion prevents alcohol-dependence induced escalation in drinking[43, 44]. Increases in proinflammatory cytokines are associated with stress and anxiety-like behavior[45, 46]. Additionally, brain-derived neurotrophic factor (BDNF) in stress regions is involved in the reduction of alcohol-induced anxiety-like behavior and microglial proinflammatory signaling in rodents[47, 48]. However, it is not known if proinflammatory microglial activation directly promotes alcohol-related hyperkatifeia. Further, proinflammatory microglial activation is associated with neurodegeneration in regions such as the prefrontal and orbitofrontal cortices that are associated with decision making, valuation, and

behavioral flexibility. However, it has not been directly determined if proinflammatory microglia drive neuronal death in these regions. Given the association between alcohol and proinflammatory signaling, and the relationship between proinflammatory signaling and negative affect, we hypothesized that proinflammatory microglia promote alcohol-induced hyperkatifeia and neurodegeneration.

In this study we assessed alcohol-induced proinflammatory activation, hyperkatifeia and neurodegeneration after two durations of binge ethanol exposures (4 or 10 binges). We assessed neuronal activity and proinflammatory vs trophic balance in stress regions involved in alcohol-related negative affect. Anxiety-like behavior and extinction of conditioned fear memory were assessed as measures of hyperkatifeia and behavioral flexibility in addition to their potential relationship to relapse and related mood disorders. To determine microglia's specific role in these proinflammatory and anxiety-like states, we targeted microglial inhibition with Gi coupled designer receptors exclusively activated by designer drugs (DREADDs) during binge ethanol as we, and others, have used previously to blunt microglial responses[49-51]. We found that binge ethanol causes acute and persistent inflammatory and microglial activation, anxiety-like states, and enhanced fear memory. These effects were prevented by Gi DREADD inhibition of microglia during binge alcohol, implicating microglia as a key driving force in promoting alcohol-induced hyperkatifeia and neurodegeneration.

Materials and Methods:

Animal models

C57/B6J wild type (WT) mice purchased from the Jackson Laboratory. For Gi DREADD inhibition, CX3CR1.Cre^{ERT2}.hM4di mice were bred in-house from CX3CR1.Cre^{ERT2} and DIO.hm4di mice (Jackson labs). All pups were weaned at 28 days old and group-housed with same-sex littermates. Animal protocols were in strict accordance with NIH regulations (Protocols 23-230.0 and 23-149.0) and approved by the University of North Carolina at Chapel Hill Institutional Animal Care and Use Committee (IACUC).

Binge ethanol treatment

Adult WT mice were administered daily intragastric (i.g.) doses of either isocaloric maltose dextran solution (9g/kg)[52] or alcohol (i.e., ethanol, 5g/kg/d) for 10 consecutive days to model human binge drinking. This dose was chosen because it produces binge level blood alcohol concentrations (BACs) over a 24-hour period equivalent to 1.4g/kg in humans (AUC: 230.7mM x hour, ~5-7 standard drinks)[53]. No weight differences were found between treatment groups. Mice were sacrificed either 24hrs after the final dose during withdrawal or 5 weeks into abstinence after behavioral testing.

Organotypic Brain Slice Culture

Organotypic brain slice cultures (OBSCs) were generated from CX3CR1.Cre^{ERT2}.hM4di mice using our standard protocols[54-56] with approval of the UNC Institutional Animal Care Use Committee (IACUC Protocol 24–096). OBSCs were prepared from P7 mouse brain based on Stoppini et al (1991) with our modifications[50-52]. Briefly, pups were decapitated and the hippocampal-entorhinal complex dissected while in Gey's buffer (Sigma-Aldrich, St. Louis, MO). Slices were then prepared by transversely cutting the regions with McIlwain tissue chopper (375

μm thickness), placed onto a membrane inserts, with 10–13 slices/ insert. Slices were maintained in MEM containing HEPES (25 mM) and Hank's salts, with 25% horse serum (HS), 5.5 g/L glucose, and 2 mM L-glutamine for 7 days in vitro, followed by 4DIV in MEM + 12% HS, and then MEM + 6% HS. To induce Cre recombination, 4-hydroxy tamoxifen (4-OH-TAM) was added 24 hours prior to experimentation. Cell death was measured with propidium iodide (PI) labeling as we have done previously[55].

Microglial Gi DREADD inhibition in vivo

Heterozygous CX3CR1.Cre^{ERT2}.hM4di were administered tamoxifen (75 mg/kg/d, i.p.) once daily for 5 days at 12 weeks of age. Mice were given 4 weeks for repopulation of peripheral monocytes before being treated with water or ethanol (5g/kg/d, i.g.) for 10 days +/- CNO (3mg/kg, 10 hours after ethanol). Mice were sacrificed 24hrs after the final dose or after 5 weeks of behavioral testing.

Perfusion and tissue collection for immunohistochemistry

Following the final dose or completion of behavioral testing, mice were sacrificed by cardiac perfusion with cold 0.1 M phosphate-buggered saline (PBS). Brains were removed from the skull and hemisected or taken whole. If hemisected, one hemisphere was dissected for cortex and hippocampus prior to being snap-frozen in liquid nitrogen for protein and RNA analysis. The contralateral hemisphere was drop-fixed in paraformaldehyde (4.0%) for immunohistochemistry. Coronal sections were made uisng a sliding microtome (40 μm, MICROM HM450; ThermoScientific, Austin, TX). Serial sections were placed in 12-well plates and stored in cryoprotectant (30% glycol/30% ethylene glycol in PBS) at -20°C.

mRNA isolation and RT-PCR

mRNA was isolated from frozen cortex or hippocampal tissue consistent with previous reporting[57]. Samples were homogenized with Trizol (Invitrogen), and RNA was isolated by chloroform extraction. The nanodrop 2000™ spectrophotometer was used to quantify RNA concentration and reverse transcription was completed with 10μL of diluted RNA and 40μL of reverse transcription mix. SYBR green PCR master mix (Applied Biosystems; 4368702) was used to complete qRT-PCR. Primer sequences were found using the PrimerBank database or designed using the National Library of Medicine Primer-BLAST tool. Housekeeping genes 18S and β-actin were used to normalize expression of genes of interest using the cycle threshold (Ct) values obtained for each product. The ddCt method was used to compare relative differences between groups and the percent change relative to 18S were used in analysis.

Protein isolation and Western Blot

Protein isolation and Western blot were performed as previously described[57]. Frozen cortex or hippocampal tissue was homogenized in Tris lysis buffer (Sucrose, 7.4% EDTA, 3.8% EGTA, 1% Triton X-100, protease, and phosphatase inhibitors, pH 7.5). Lysates were centrifuged at 21,000g for 40 minutes and supernatants were diluted in RIPA and protease inhibitor (1:100, Sigma Aldrich; R0278, P8340). Protein (40mg) was loaded into each lane on Mini-PROTEAN TGX Stain-Free Gels (BioRad; 4568124) and ran on 140 volts before being transferred to PVDF membranes (BioRad; 1704158). Membranes were washed in TBS and blocked for 1 hour at room temperature (LI-COR Blocking Solution; 92760001) before overnight incubation at 4°C in primary

antibodies. The following day, membranes were washed in TBS with 0.1% Tween-20 (Sigma Aldrich; P2287) and incubated in the corresponding conjugated secondary antibody (LI-COR). Membranes were washed in TBS then scanned using LI-COR Image Studio Lite Version 5.2. Positively stained bands were analyzed using the Image Studio Lite software with proteins of interest normalized to a housekeeping protein such as GAPDH.

Immunohistochemistry (IHC) and immunofluorescence (IF) staining

Immunohistochemistry staining was performed consistent with previous reporting[57]. For immunohistochemistry (IHC), free-floating tissue sections (40 µm) were washed in 0.1M PBS, quenched in 0.6% H_2O_2 for 30 minutes to inhibit endogenous peroxidases, then incubated for 1 hour at 70°C in pH=6.0 1X Antigen Retrieval Citra solution (Fisher; NC9935936). For membrane permeability, sections were blocked at room temperature for 1 hour in 4% normal serum with 0.1% Triton X-100 (Millipore Sigma; T8787). Sections were incubated in primary antibody in blocking solution overnight at 4°C. Sections were then washed in PBS and incubated in the corresponding biotinylated secondary antibody (1:200, Vector Laboratories) for 1 hour at room temperature. Following another wash, the sections were incubated in avidin-biotin complex (Vector Vectastain ABC Kit; PK-6100) for 1 hour. 3,3'-Diaminobenzidine tetrahydrochloride hydrate (Sigma-Aldrich; D4293-50SET) was used for visualization. Sections were then mounted on glass slides, allowed to dry, dehydrated in a series of ethanol concentrations, and covered using Cytoseal (Fisher; 22-050-262).

For immunofluorescence staining (IF), tissue sections were washed in PBS then incubated for 1 hour at 70°C in 1X Citrate Buffer for antigen retrieval. This was followed by a PBS wash and blocking at room temperature for 1 hour in 8% normal serum with 0.1% Triton X-100 before overnight incubation in relevant primary antibody at 4°C. The following day, sections were washed and incubated at room temperature in the corresponding Alexa Fluor conjugated secondary antibody (1:1000; Invitrogen). Sections were washed and mounted, allowed to dry, and cover slipped with Prolong Gold Anti-Fade mounting medium with DAPI (ThermoFisher; P36971). Representative images of the tissue were taken on the Keyence BZ-X800 Microscope and accompanying software was used for microscopic analysis. For each region of interest, images were taken of ~3 identical sections per subject, selected by desired bregma according to the mouse brain atlas (Paxinos and Watson). By regions, bregmas were: infralimbic cortex (IL, 1.98mm), medial prefrontal cortex (mPFC, 2.10 mm), orbital frontal cortex (OFC, 2.10mm), dorsal and ventral bed nucleus of the stria terminalis (BNST, 0.14mm), central amygdala (CeA, -1.82mm), and basal lateral amygdala (BLA, -1.70mm) Staining was reported in pixels/mm^2.

Behavioral assessments

Open field. Exploratory activity in a novel environment was assessed by a one-hour trial in an open field chamber (41 cm x 41 cm x 30 cm) crossed by a grid of photobeams (VersaMax system, AccuScan Instruments). Counts were taken of the number of photobeams broken during the trial, with separate measures for locomotor activity (total distance traveled) and vertical rearing movements. Time spent in the center region was used as an index of anxiety-like behavior.

Acoustic startle test. This procedure was used to assess auditory function, reactivity to environmental stimuli, and sensorimotor gating. The test was based on the reflexive whole-body flinch, or startle response, which follows exposure to a sudden noise. Measures were taken of startle magnitude and prepulse inhibition, which

occurs when a weak prestimulus leads to a reduced startle in response to a subsequent louder noise (San Diego Instruments SR-Lab system). Mice were placed into individual small Plexiglas cylinders within larger, sound-attenuating chambers. Each cylinder was seated upon a piezoelectric transducer, recording the force of startle responses. The chambers included a ceiling light, fan, and a loudspeaker for the acoustic stimuli. Each session began with a five-min habituation period, followed by 42 trials (7 of each type): no-stimulus trials, trials with the acoustic startle (40 msec; 120 dB) alone, and trials with a prepulse stimulus (20 msec; either 74, 78, 82, 86, or 90 dB) occurred 100 msec before the onset of the startle stimulus. Measures were taken of the startle amplitude for each trial across a 65-msec sampling window, and an overall analysis was performed for each subject's data for levels of prepulse inhibition at each prepulse sound level (calculated as 100 - [(response amplitude for prepulse stimulus and startle stimulus together / response amplitude for startle stimulus alone) x 100].

Morris water maze. The water maze was used to assess spatial and reversal learning, swimming ability, and vision. The water maze consisted of a large circular pool (diameter = 122 cm) partially filled with water (45 cm deep, 24-26o C), located in a room with numerous visual cues. The procedure involved two 5-day phases: acquisition in the hidden platform task, and a test for reversal learning (an index of cognitive flexibility). In both phases, mice were tested for their ability to find a submerged, hidden escape platform (diameter = 12 cm). For each trial, the mouse was placed in the pool at 1 of 4 possible locations (randomly ordered), and then given 60 sec to find the platform. If the mouse found the platform, the trial ended, and the animal was allowed to remain 10 sec on the platform before the next trial began. If the platform was not found, the mouse was placed on the platform for 10 sec, and then given the next trial. Measures were taken of latency to find the platform and swimming speed via an automated tracking system (Noldus Ethovision). 2-3 hours after the final trial on day 5, mice were given a 1-min probe trial in the pool with the platform removed. Selective quadrant search was evaluated by measuring percent time in the quadrant where the platform (the target) had been located during training and number of crosses over the platform area, versus the corresponding areas in the other three quadrants. Following the acquisition phase, mice were tested for reversal learning, using the same procedure as described above. In this phase, the hidden platform was re-located to the opposite quadrant in the pool. As before, measures were taken of latency to find the platform. On day 5 of testing, the platform was removed from the pool, and the group was given a probe trial to evaluate reversal learning.

Conditioned fear. This standard test for learning, memory, and extinction was conducted across 3 days, using a Near-Infrared image tracking system (MED Associates, Burlington, VT). On the first day, mice were given a 7-min training session. Mice were placed in the test chamber, contained in a sound-attenuating box, and allowed to explore for 2 min. The mice were then exposed to a 30-sec tone (80 dB), which co-terminated with a 2-sec scrambled foot shock (0.4 mA). Mice received 2 additional shock-tone pairings during the training session. Context-dependent learning was evaluated on the second day of testing. Mice were placed back into the original test chamber, and levels of freezing (immobility) were determined across a 5-min session. On the third day of testing, mice were evaluated for associative learning to the auditory cue and extinction of freezing responses. To conceal contextual cues, the conditioning chambers were modified using a Plexiglas insert to change the wall and floor surface, and a mild novel odor (70% ethanol) was added to the sound-attenuating box. Mice were

placed in the modified chamber and allowed to explore. After 2 min, mice were given 50 presentations of the 30-sec tone, with 5 sec between each presentation. Levels of freezing before and during the stimuli were obtained by the image tracking system.

Statistical analyses

Statistical tests were performed in GraphPad Prism™. *t*-tests were used for preplanned orthogonal contrasts. 1-way or 2-way ANOVAs were used for multiple-group assessments. Sidak's post-tests were used when appropriate. Outliers were detected and removed according to Grubb's test. *P*-values less than 0.05 were considered significant.

Results

Binge ethanol acutely induces proinflammatory signaling and cortical neuronal death.

Studies in postmortem human brain suggest the extent of proinflammatory activation is related to the lifetime duration of alcohol use. To test this directly, we assessed proinflammatory activation and neuronal death in mice after 4 or 10 daily consecutive alcohol binges. Mice received 5g/kg/d by gavage to model human binge drinking as reported previously[58]. Mice metabolize alcohol (i.e., ethanol) up to 10X faster than humans[53]. Thus, in mice this dose results in a blood ethanol concentration AUC x time of 230.7mM x hour, which is seen in humans with ~1.4g/kg or ~7 drinks (14g standard drink, 70kg body weight)[53]. Twenty-four hours after ten alcohol binges, increases in proinflammatory gene expression were seen in the cortex of males and females, including cytokines IL-1α, IFNγ, and TRAIL, along with decreases in the resting microglial state markerTMEM119 (Figure 1A). In addition to these gene changes, microglial phenotypes were also significantly altered in stress-related regions with greater changes seen with longer binge duration (Figure 1B-M). The IL, BNST, and CeA, were assessed due to these regions' involvement in negative-affect states[24-28]. In the male IL, Iba-1 staining revealed decreased microglial area (cell body and processes) with 10 binges, consistent with a strongly activated, phagocytic state (Figure 1B-C). The female IL also showed a hyper-ramified activation state after 10 binges with increased microglial Iba-1 area (Figure 1D-E). In the male vBNST microglia were strongly activated, with decreased cell body and processes at 10 days (Figure 1F-G), with no changes were seen in the female vBNST (Figure 1H-I). In the dBNST no changes were seen in males (Figure 1J-K) , though significant activation was seen in females with 10 alcohol binges (Figure 1L-M). In the CeA, a different pattern was observed with both males and females showing decreases in microglial area at day 4, returning to original control levels at day 10 (Supplemental Figure 1A,B). Assessments of the effects of binge ethanol on neurodegeneration in the OFC and mPFC showed increased robust increases in the executioner capsase-3 that reached a peak after 4 binges in the OFC, but steadily increased from 4 to 10 binges in the mPFC (Figure 1N-O). Definitive assessment of cell death by TUNEL, found positive staining only in the OFC that was increased with 10 alcohol binges (Figure 1P-Q). Thus, binge alcohol as region and sex-specific effects on microglial activation and neurodegeneration. Generally, the level of proinflammatory activation increased with the number of binges. Considering these changes in proinflammatory activation and neuronal death, we next assessed the effect of binge alcohol on trophic support in these regions.

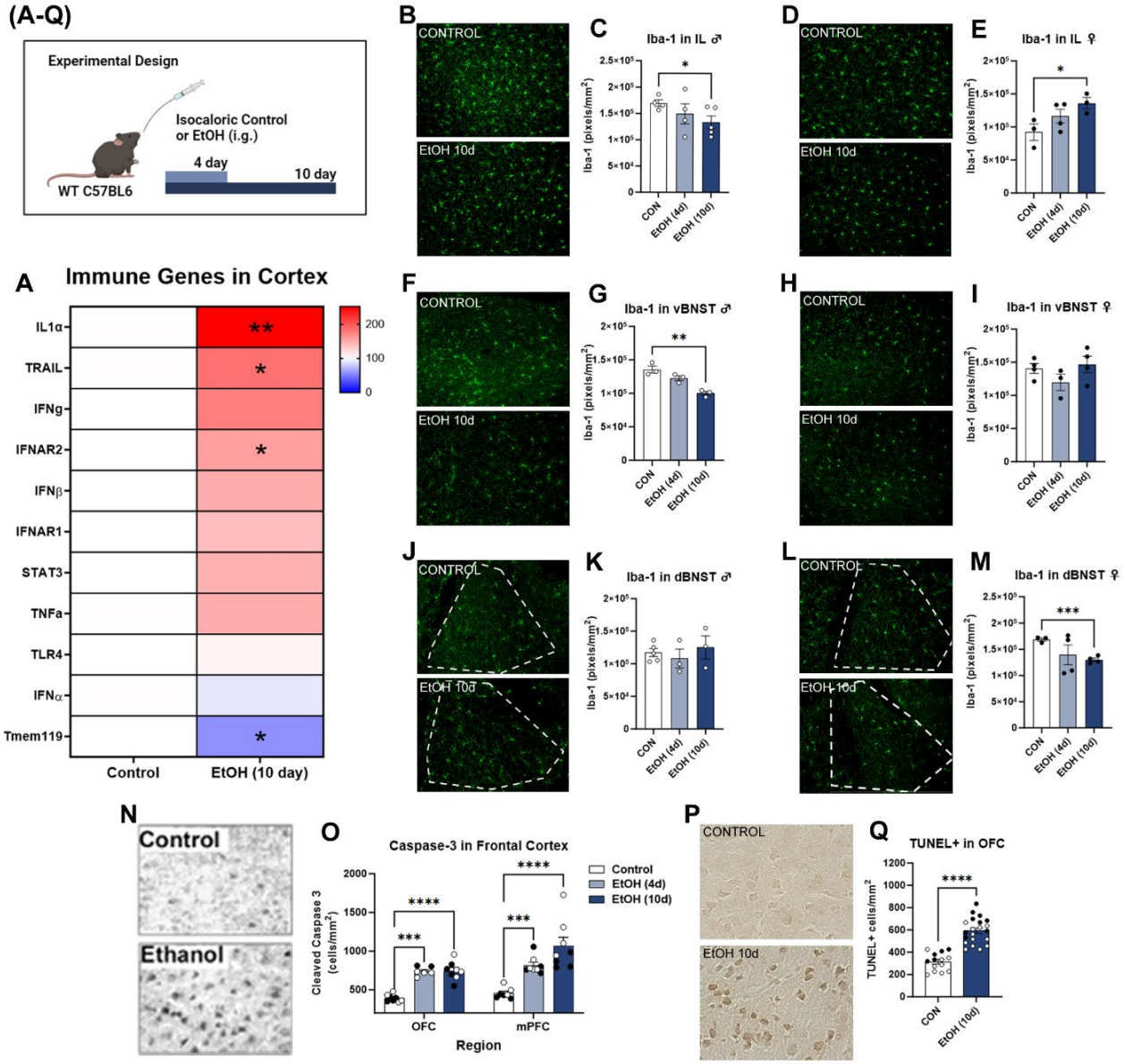

Figure 1: Acute proinflammatory activation with binge alcohol. Mice received isocaloric maltose dextran (9g/kg/d, i.g.) or binge ethanol treatment (5g/kg/d, i.g.) for 4 or 10 days with assessments 24 hours after the last treatment. Sexes were combined when no sex effects were observed. Males-open circles, females-black circles. **(A)** Proinflammatory gene expression in both males and females at 10 days of ethanol (N= Control=5 males, 5 females; 10-day ethanol=4 males, 4 females). **(B-M)** Iba-1 IHC for microglia morphology. (N= Control=5 males, 5 females; 4-day ethanol=5 males, 5 females, 10-day ethanol=5 males, 4 females). **(B)** Representative images of Iba-1 in male IL. **(C)** Ethanol caused proinflammatory activation in the IL of males seen by reduced microglial cell body and process area that reached significance with 10 days of binge ethanol. *$p<0.05$. **(D)** Representative images of Iba-1 in female IL. **(E)** Ethanol caused a hyper-ramified proinflammatory activation state in the IL of females seen by increased microglial area that reached significance with 10 days of binge ethanol. *$p<0.05$. **(F)** Representative images of Iba-1 in male vBNST. **(G)** Ethanol caused proinflammatory activation in the male vBNST seen by reduced microglial cell body and process area that reached significance with 10 days of binge ethanol. **$p<0.01$. **(H)** Representative images and **(I)** quantification of Iba-1 in female vBNST showed no change. **(J)** Representative images and **(K)** quantification of Iba-1 in male dBNST showed no change. **(L)** Representative images of Iba-1 in female dBNST. **(M)** Ethanol caused proinflammatory activation in the dBNST of females seen by reduced microglial cell body and process area that reached significance with 10 days of binge ethanol. ***$p<0.001$. **(N)** Representative images and **(O)** quantification of increased cleaved caspase-3 stain in the OFC (~2-fold) at 4 and 10 days, and mPFC (~2-fold) at 4 days and (~2.75-fold) 10 days of treatment. **(P)** Representative images and **(Q)** quantification of increased TUNEL cell death stain in the OFC (~2-fold) with 10 days of ethanol treatment in both males and females.

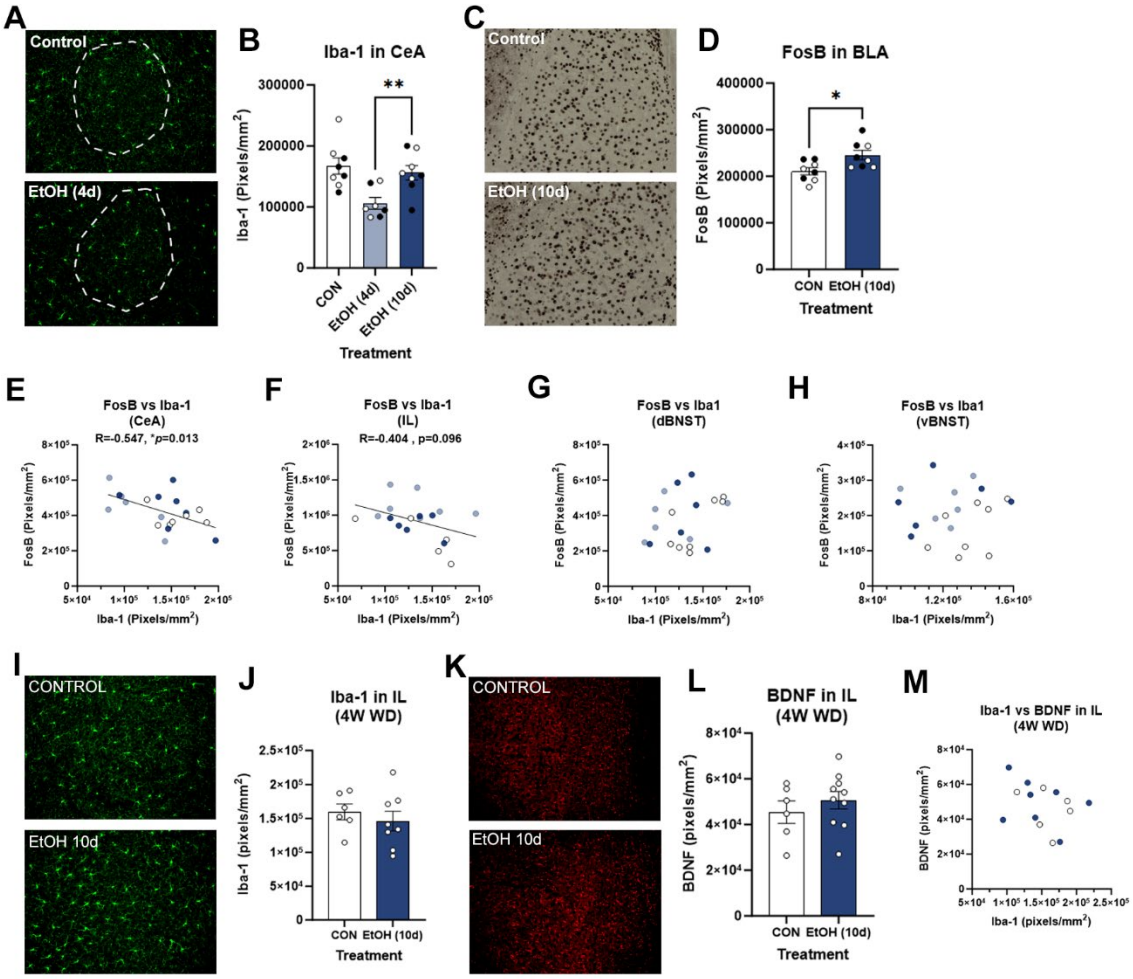

Supplemental Figure 1. Disrupted microglial phenotype and increased neuronal activity with binge ethanol. Mice received isocaloric control (9g/kg/d, i.g.) or binge ethanol treatment (5g/kg/d, i.g.) for 4 or 10 days with assessments 24 hours after the last treatment**.** (N= Control=5 males, 5 females; 4-day ethanol=5 males, 5 females, 10-day ethanol=5 males, 4 females). **(A)** Representative images and **(B)** quantification for Iba-1 in the CeA show a decrease in microglia cell body and processes at 4 days, with a return to isocaloric levels by 10 days of binge ethanol $**p<0.01$. **(C-D)** FosB IHC for neuronal activation. Males-open circles, females-black circles. **(C)** Representative images and **(D)** quantification for increased FosB in the BLA of both males and females show increased neuronal activation at 10 days of treatment $*p<0.05$. **(E-H)** Correlations for FosB vs Iba-1 for neuronal activation vs microglia activation. Open circles = isocaloric control, light blue circles = 4-day EtOH, dark blue circles = 10-day EtOH. **(E)** In the CeA, a negative correlation was seen between FosB and Iba-1, with increased decreased microglial cell body and processes correlating to decreased neuronal activation. R=-0.547, $*p=0.013$. **(F)** A negative trend was observed between FosB and Iba-1 expression in the IL, linking increased microglial size with decreased neuronal firing. R=-0.404, $p=0.096$. No correlation was observed between FosB and Iba-1 in the **(G)** dBNST and **(H)** vBNST. **(I-M)** Iba-1 and BDNF IHC in the IL. **(I)** Representative images and **(J)** quantification for Iba-1 in the IL show no change. **(K)** Representative images and **(L)** quantification for BDNF in the IL show no change. **(M)** No correlation was observed between Iba-1 and BDNF in the IL.

Binge ethanol causes a loss of BDNF and promotes neuronal excitation in stress-related regions.

Since binge ethanol acutely induced proinflammatory activation and neuronal death in stress-related regions, we next assessed the effects of 10-day binge ethanol on neuronal activation and trophic support. To evaluate neurotrophic changes resulting from binge ethanol, we measured BDNF levels in similar stress-related regions. In both male and female dBNST 10 ethanol binges significantly decreased BDNF compared to controls (Figure 2A-B). Likewise, in the CeA both sexes showed a hint toward a slight increase in BDNF after 4 binges that was significantly reduced with 10 alcohol binges (Figure 2C-D). No differences were seen in the vBNST (Figure 2E-F). In the IL males showed no change in BDNF, though the females had significantly increased BDNF expression at 4 days of treatment, which then significantly decreased at day 10 (Figure 2G-H).

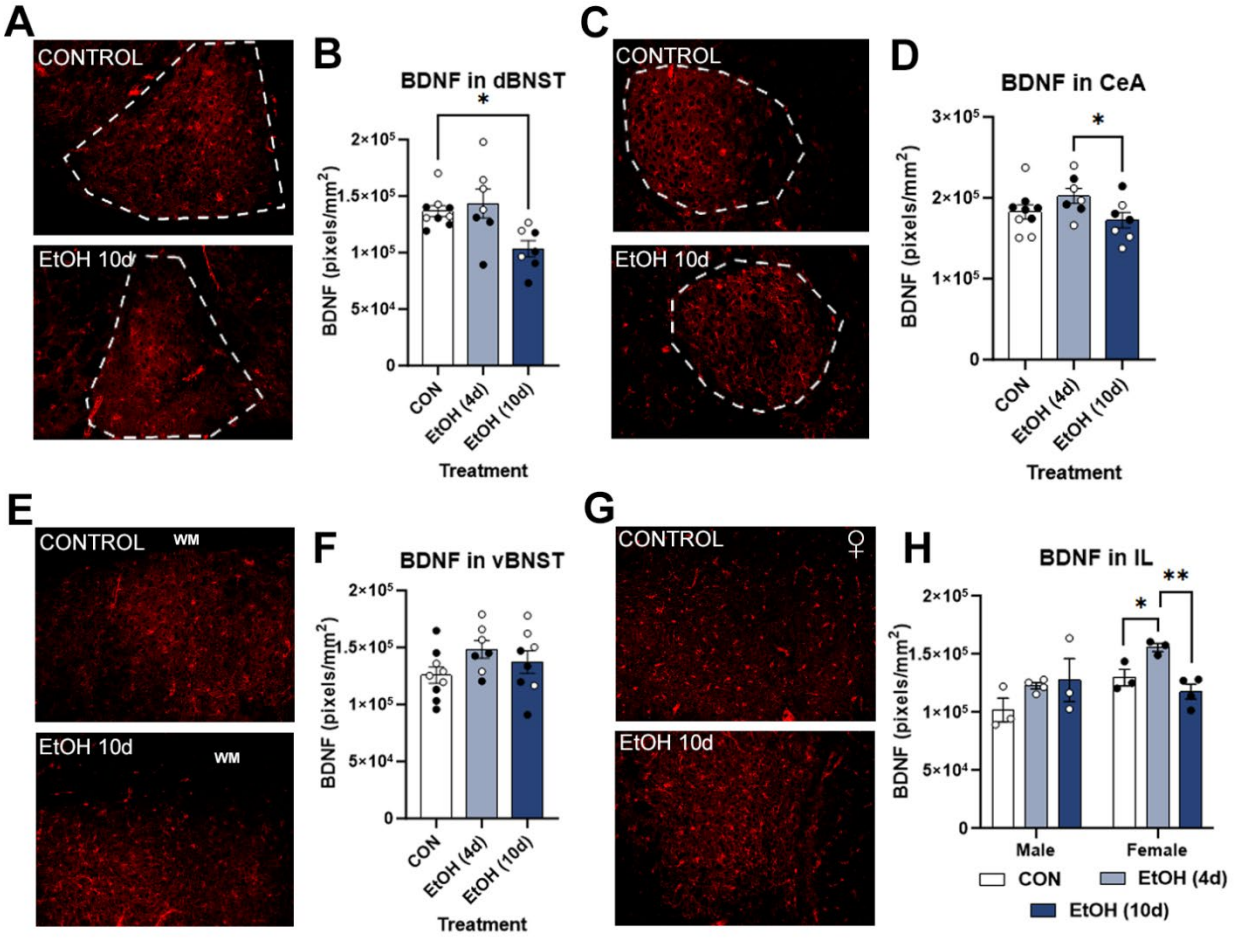

Figure 2. Loss of trophic support with binge ethanol. Mice received isocaloric control or binge ethanol treatment (5g/kg/d, i.g.) for 4 or 10 days with assessments 24 hours after the last treatment. (N= Control=5 males, 5 females; 4-day ethanol=5 males, 5 females, 10-day ethanol=5 males, 4 females). **(A-H)** BDNF IHC for trophic support. Males-open circles, females-black circles. **(A)** Representative images of BDNF in the dBNST. **(B)** Ethanol caused a decrease in trophic support in the dBNST of males and females that reached significance at 10 days. *$p<0.05$. **(C)** Representative images of BDNF in CeA. **(D)** Ethanol caused a decrease in trophic support from 4 to 10 days in the CeA, seen by decreased BDNF. *$p<0.05$. **(E)** Representative images of BDNF in vBNST, **(F)** with no change in BDNF seen. **(G)** Representative images of BDNF in IL. **(H)** In the female IL, ethanol slightly increased BDNF at 4 days, with no change at 10 days of treatment. $p=0.086$. In the male IL, BDNF increased with ethanol at 4 days, but significantly decreased trophic support was seen at 10 days *$p<0.05$, *$p<0.01$. WM: white matter.

Considering the effects of binge ethanol on proinflammatory activation and loss of trophic support, we then assessed FosB as a measure of neuronal activation over the prior 24 hours in these stress regions. In the dBNST of both sexes, FosB was significantly increased by day 10 (Figure 3A-B). The male vBNST showed similar effects, with significant increases in FosB observed at day 4 and 10, though no significant change was seen in the females (Figure 3C-D). The CeA of both sexes also showed increases in FosB at 10 days of binge ethanol (Figure 3E-F). FosB analysis was also assessed in the BLA, since this region is thought to be involved with anxiety-like behavior[59]. In the BLA, FosB was significantly increased after 10 alcohol binges (Supplemental Figure 1C-D). In the male IL, FosB was significantly increased with 4 and 10 binges, with the female IL showing increases with 4, but a return to control levels after 10 binges (Figure 3G-H). We then assessed the correlations of FosB expression between the stress regions, as they are known to form functional circuits in AUD and found significant correlations between the vBNST and IL, as well as the vBNST and dBNST (Figure 3I). To assess for a possible link between trophic support and neuronal activation, we assessed correlations between BDNF and FosB across regions. In the dBNST and CeA significant negative correlations were found between FosB and BDNF (Figure 3J-K). Further, we assessed relationships between neuronal activation and microglia activation.

A significant negative correlation was found between FosB and Iba-1 in the CeA (Supplemental Figure 1J). In the IL, there was a negative trend between FosB and Iba-1 that did not reach significance (Supplemental Figure 1G). No correlations were observed in the dBNST and vBNST (Supplemental Figure 1G,H). Considering these neuronal and trophic changes in stress-related regions during immediate withdrawal from binge ethanol, we then assessed how these effects extend into periods of abstinence.

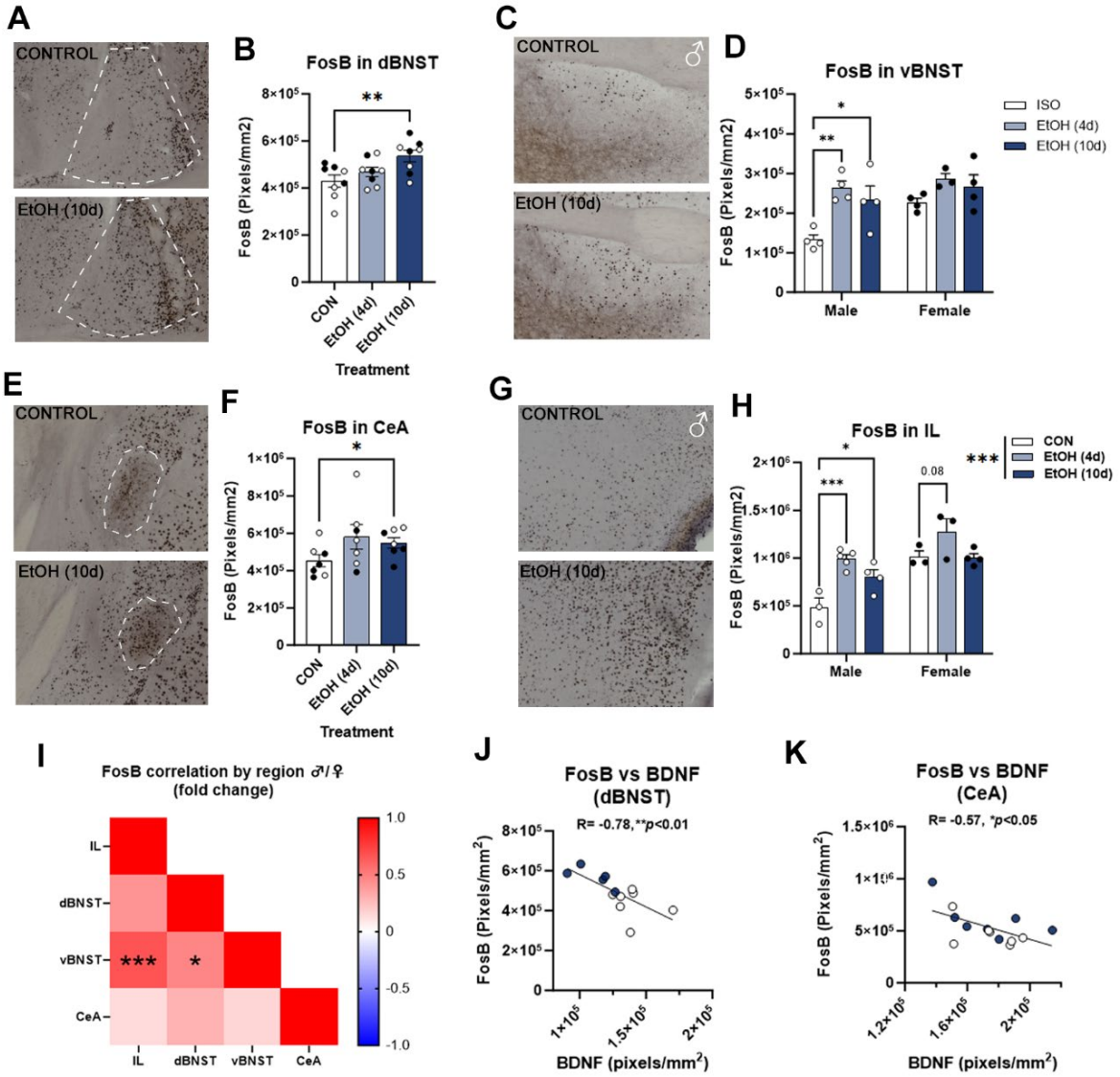

Figure 3. Increased neuronal activity with binge alcohol. Mice received isocaloric control (9g/kg/d, i.g.) or binge ethanol treatment (5g/kg/d, i.g.) for 4 or 10 days with assessments 24 hours after the last treatment**. (A-H)** FosB IHC for neuronal activity. Males-open circles, females-black circles. **(A)** Representative images and **(B)** analysis of FosB in dBNST show heightened neuronal activation in response to ethanol, seen by increased FosB in males and females that reached significance at 10 days. $^{**}p<0.01$. . **(C)** Representative images of FosB in vBNST. **(D)** Ethanol caused significantly increased neuronal activity in the vBNST of males at 4 and 10 days. $^{**}p<0.01$, $^{*}p<0.05$, Sidak's post-test. No change was seen in the female vBNST. **(E)** Representative images and **(F)** analysis of FosB in CeA show increased neuronal activation in both males and females at 10 days of ethanol. $^{*}p<0.05$. **(G)** Representative images of FosB in IL. **(H)** Ethanol caused increased neuronal activity in the IL of males seen at 4 and 10 days of binge alcohol. $^{***}p<0.001$, $^{*}p<0.05$, Dunnett's post-test. Ethanol disrupted neuronal activation at 4 days of treatment with no changes seen at 10 days in the female IL. $p=0.08$ **(I)** Heat map of FosB correlations between regions show significant positive correlations between FosB in the IL and vBNST, and dBNST and vBNST. $^{***}p<0.001$, $^{*}p<0.05$. Sexes were combined. **(J-K)** Correlations between FosB and BDNF IHC for neuronal firing versus trophic support at 10 days of treatment. Sexes were combined. Control=open circles, 10-day ethanol=black circles. **(J)** Neuronal firing correlated negatively with trophic support in the dBNST, seen by a negative correlation between FosB and BDNF. R=-0.78, $^{**}p<0.01$. **(K)** FosB was negatively correlated with BDNF in the CeA, suggesting decreased trophic support with increased neuronal activation. R=-0.57, $^{*}p<0.05$. N= Control:5 males, 5 females; 4-day ethanol: 5 males, 5 females, 10-day ethanol: 5 males, 4 females.

Binge ethanol causes persistent proinflammatory activation and loss of trophic support.

Due to the immediate heightened proinflammatory and neurotrophic loss of binge ethanol in stress-related regions 24 hours into withdrawal, we then assessed how these changes persisted through a period of abstinence.

Following 4 weeks of abstinence from 10 daily ethanol binges, microglia were persistently hyperactivated in the dBNST, seen by decreased area of microglia cell body and processes (Figure 3A-B). In the dBNST reductions in BNDF were found with a trend toward statical significance threshold of 0.05 (Figure 4C-D). No significant correlation was found between Iba-1 and BDNF in the dBNST (Figure 4E). In the vBNST, Iba-1 was also significantly decreased 4 weeks into withdrawal (Figure 4F-G), with no change was seen in BDNF (Figure 4H-I), and no correlation was observed between the two (Figure 4J). Signs of a hyper-ramified state were seen in the CeA with trend toward significantly increased Iba-1 (Figure 4K-L), with a significant reduction in BDNF at this time point (Figure 4M-N). Iba-1 and BDNF levels in the CeA showed a trend toward a negative correlation (Figure 4O). In the IL, no persistent changes in Iba-1 or BDNF were seen with no correlation between the two (Supplemental Figure 1I-M). Thus, persistent pro-inflammatory microglial activation and decreased BDNF was found in certain key stress-related regions such as the BNST and CeA. This led us to question the behavioral effects of binge ethanol during withdrawal.

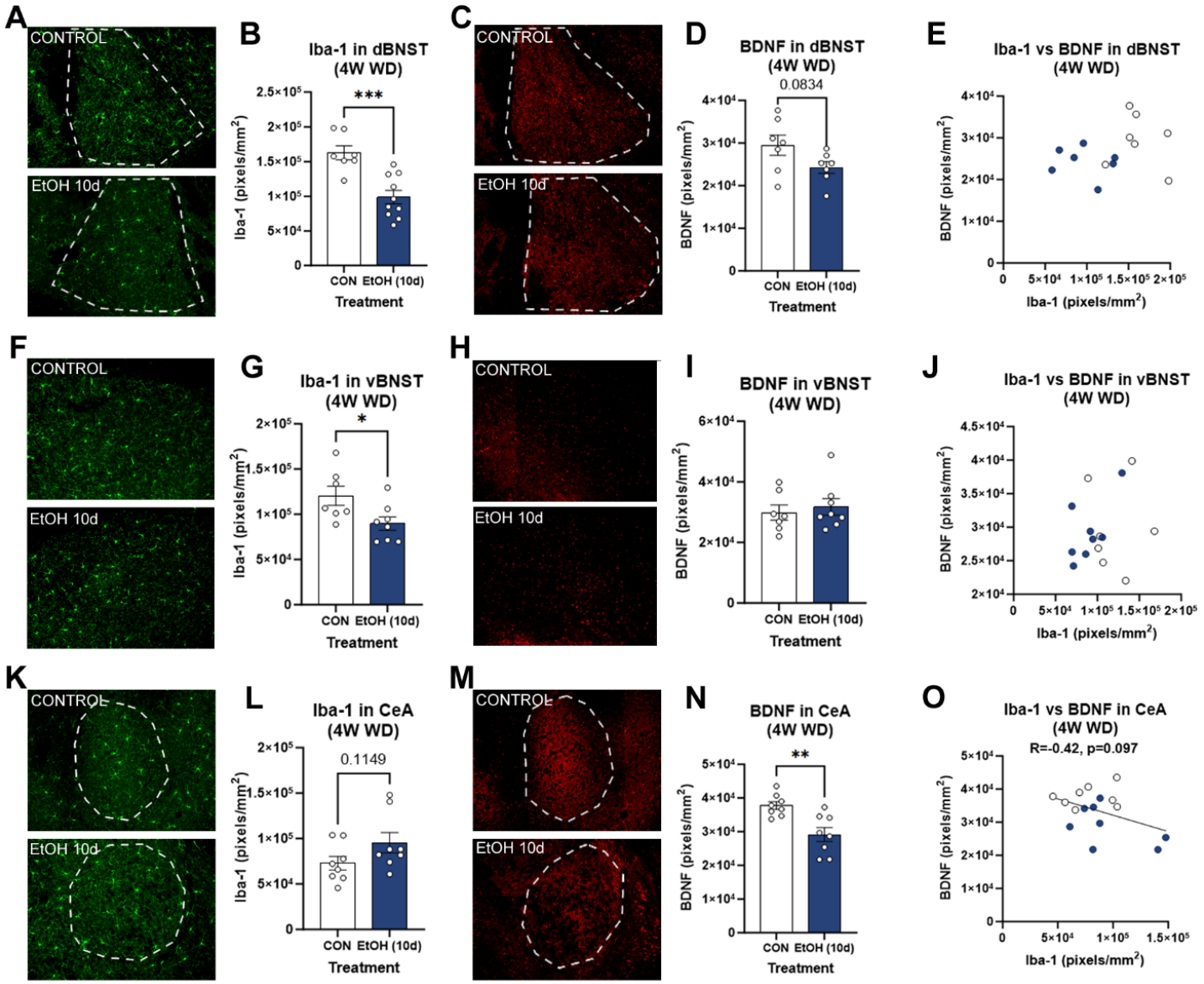

Figure 4. Persistent changes in microglia and BDNF with binge alcohol. Following 10-day binge ethanol treatment with isocaloric control (9g/kg/d, i.g.) or binge alcohol (5g/kg/d, i.g.) and behavioral testing, IHC assessments were completed four weeks into withdrawal. (N= Control=10 males, 4-day ethanol=12, 10-day ethanol=10

males). **(A-E)** Iba-1 and BDNF IHC in the dBNST. **(A)** Representative images of Iba-1 in the dBNST. **(B)** Ethanol caused persistent proinflammatory activation in the dBNST seen by decreased microglial cell body and processes. ***$p<0.001$. **(C)** Representative images and **(D)** quantification for BDNF in the dBNST show decreased trophic support with binge ethanol 4 weeks into withdrawal. $p=0.083$. **(E)** No correlation was observed between Iba-1 and BDNF in the dBNST. **(F-J)** Iba-1 and BDNF IHC in the vBNST. **(F)** Representative images for Iba-1 in the vBNST. **(G)** Ethanol caused persistent proinflammatory activation in the vBNST seen by decreased cell body and process area that reached significance following 4 weeks of withdrawal. *$p<0.05$. **(H)** Representative images and **(I)** quantification for BDNF in the vBNST show no change 4 weeks into withdrawal. **(J)** No correlation was observed between Iba-1 and BDNF in the vBNST. **(K-O)** Iba-1 and BDNF IHC in the CeA. **(K)** Representative images for Iba-1 in the CeA. **(L)** Binge ethanol caused a persistent hyper-ramified proinflammatory activation state in the CeA seen by the increase in microglial cell bodies and processes, thought this did not reach significance. $p=0.115$. **(M)** Representative images and **(N)** quantification for BDNF in the CeA show decreased trophic support at 4 weeks of withdrawal. **$p<0.01$. **(O)** A negative trend was observed between Iba-1 and BDNF in the CeA, with increased microglial activation associated with decreased trophic support. R=-0.42, p=0.097.

Binge alcohol enhances anxiety-like behavior and fear memory during abstinence.

Due to the persistent proinflammatory activation and neuronal disruption in stress-related regions reported above, in addition to the association between hyperkatifeia and relapse, we performed behavioral analyses during abstinence to binge ethanol (Figure 5A). Open field and acoustic startle were performed to assess effects on anxiety-like behavior 3 days into withdrawal. Morris Water Maze and conditioned fear testing assessed changes in learning and fear memory at 10 and 24 days of withdrawal, respectively. Mice traveled significantly less distance in the center of the open field with 4 but not 10 ethanol binges consistent with increased anxiety-like behavior (Figure 5B). In the acoustic startle test, mice receiving 10 ethanol binge showed increased startle magnitudes across different pre-pulse decibels consistent with hyperarousal (Figure 5C). In the Morris Water Maze, mice exhibited no differences in learning (Figure 5D). The escape platform was then moved to measure reversal learning, a measure of behavioral flexibility. Ethanol binge reduced reversal learning in a dose-dependent manner seen with a right shift in the learning curve (Figure 5E) and reduced time spent in the reversal learning quadrant during the probe trial (Figure 5F). A representative path tracing illustrates this difference (Figure 5G). In Pavlovian fear conditioning, no differences were found in the acquisition of conditioned fear cue association learning. However, mice receiving 10 ethanol binges failed to extinguish the conditioned fear memory cue association, while their control and 4 ethanol binge counterparts showed clear memory extinction (Figure 5I) Thus, binge ethanol promotes anxiety-like behavior and a loss of behavioral flexibility with reduced fear memory extinction that increases with the number of binge exposures. Given these behavioral phenotypes and persistent proinflammatory/trophic imbalance with prolonged abstinence from binge ethanol, we next assessed the specific role microglia play in the development of these persistent proinflammatory and negative-affective states.

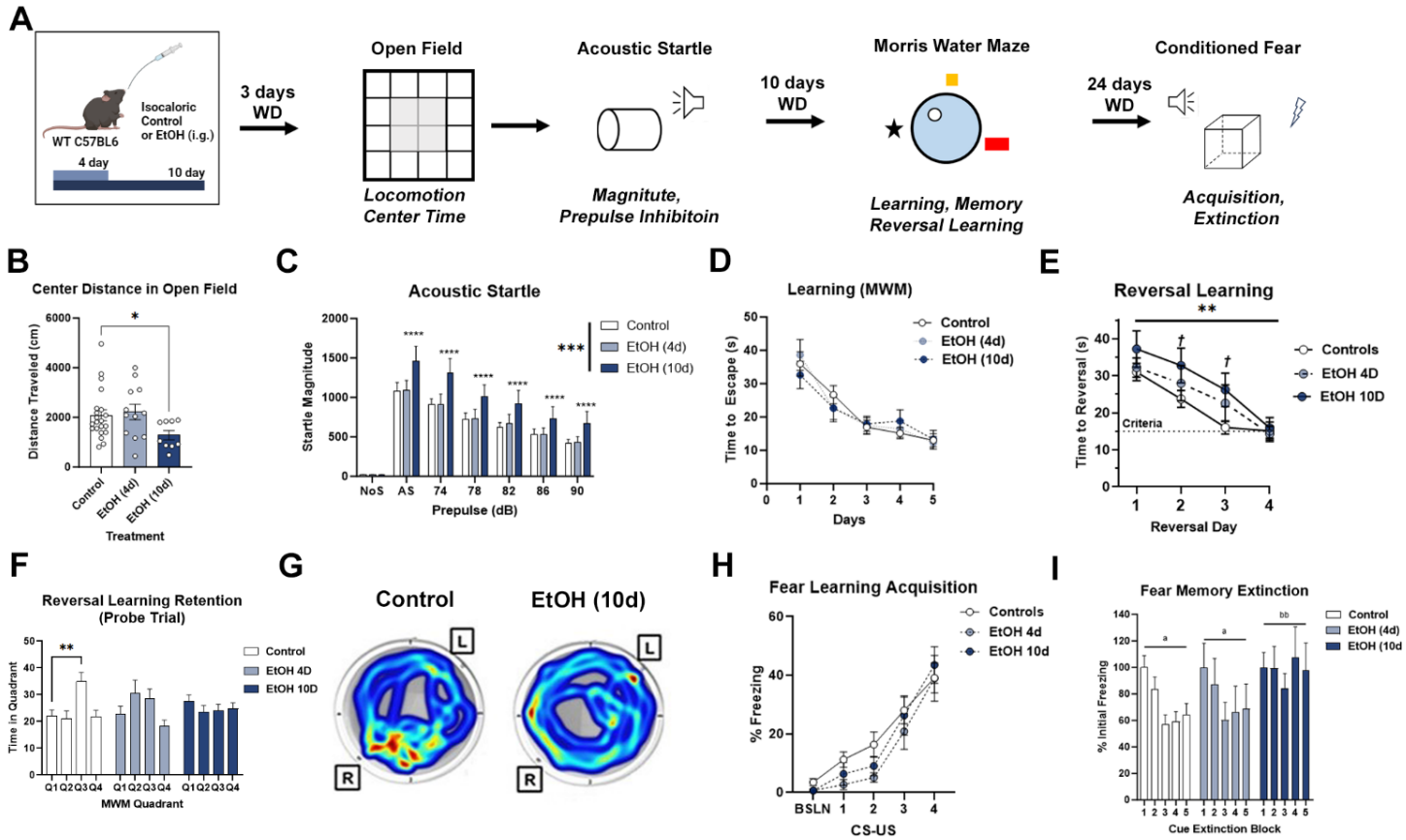

Figure 5. Negative affect and cognitive dysfunction with binge alcohol. (A) Male mice underwent behavioral testing following 4- or 10-day treatment with isocaloric control (9g/kg/d, i.g.) or binge ethanol (5g/kg/d, i.g.). (N= Control=10 males, 4-day ethanol=12, 10-day ethanol=10 males) At 3 days post-ethanol treatment, mice underwent open field testing for anxiety, followed by acoustic startle for arousal. The Morris Water Maze (MWM) testing began 10 days into abstinence for learning and reversal learning. Finally, 24 days into withdrawal, the mice underwent conditioned fear testing for acquisition and extinction. **(B)** Mice receiving 10 days of binge ethanol traveled significantly less distance in the center of the open field (cm) (*p<0.05). **(C)** Binge ethanol increased the magnitude of acoustic startle across pre-pulse intensities (dB) following 10 days of treatment. ****p<0.0001. **(D)** No change in learning with the Morris Water Maze was observed. Binge ethanol led to **(E)** increased time (s) to reversal learning. (**p<.01, Sidak's Post-test) and **(F)** reduced time spent in the reversal quadrant (Q3) in EtOH treatment groups during probe trial after reversal learning (**p<0.01, Sidak's Post-test) **(G)** Representative heat map tracing during the reversal learning probe trial showing control mice spending a greater amount of time in the correct reversal quadrant than the ethanol-treated mice. R: reversal quadrant, L: initial learning quadrant **(H)** Binge ethanol had no effect on freezing acquisition in conditioned fear learning trials. **(I)** Control and 4-day binge ethanol groups showed extinction of conditioned fear memory, while mice receiving 10 ethanol binges showed no extinction. *p<0.05, 1-way ANOVA.

Chemogenetic inhibition of microglia prevents ethanol-induced proinflammatory activation and neurodegeneration.

Considering the acute and persistent changes in microglial phenotype and ethanol-induced neuronal death and proinflammatory activation reported above, we next assessed how microglia drive these effects. To determine this, we utilized chemogenetic Gi DREADD (hM4di) inhibition of microglia. We and others have used this approach previously, as microglia mobilize intracellular calcium stores to change their effector state. To confirm microglia-specific Gi DREADD expression, we prepared OBSCs from CX3CR1.Cre^{ERT2}.hM4di.mCitrine (+/-) mice. Heterozygotes were used since the CreERT2 transgene causes a functional null mutation of CX3CR1, an important regulator of microglial activation state, in the inserted allele. Addition of 4-OH-TAM to cultures caused robust expression of the mCitrine tag within Iba-1+ microglia, consistent with microglial-specific expression of the Gi DREADD (Figure 6A). Slices were then treated with a binge concentration of ethanol (100mM) +/- CNO to activate Gi signaling in microglia. Consistent with our previous reports, ethanol increased the expression of TNFα (2-fold), IL-1β (34-fold) and MCP-1 (25-fold), proinflammatory factors associated with microglial activation[60, 61](Figure 6A-B). Induction of microglial Gi signaling with the DREADD ligand CNO blocked this

response, returning TNFα and MCP1 to control levels and blunting the IL-1β response by 63% (Figure 6B). Subsequently, Gi DREADD microglial inhibition prevented the induction of cell death by ethanol in OBSC as measured by PI uptake (Figure 6C-D). We then assessed the role of proinflammatory microglia's role in ethanol-induced neurodegeneration *in vivo* after 10 daily ethanol binges (Figure 6E). Ethanol caused robust TUNEL+ cell death in the OFC that was prevented by Gi DREADD inhibition of proinflammatory microglia revealing a critical role microglia in alcohol-induced cell death (Figure 6F-G).

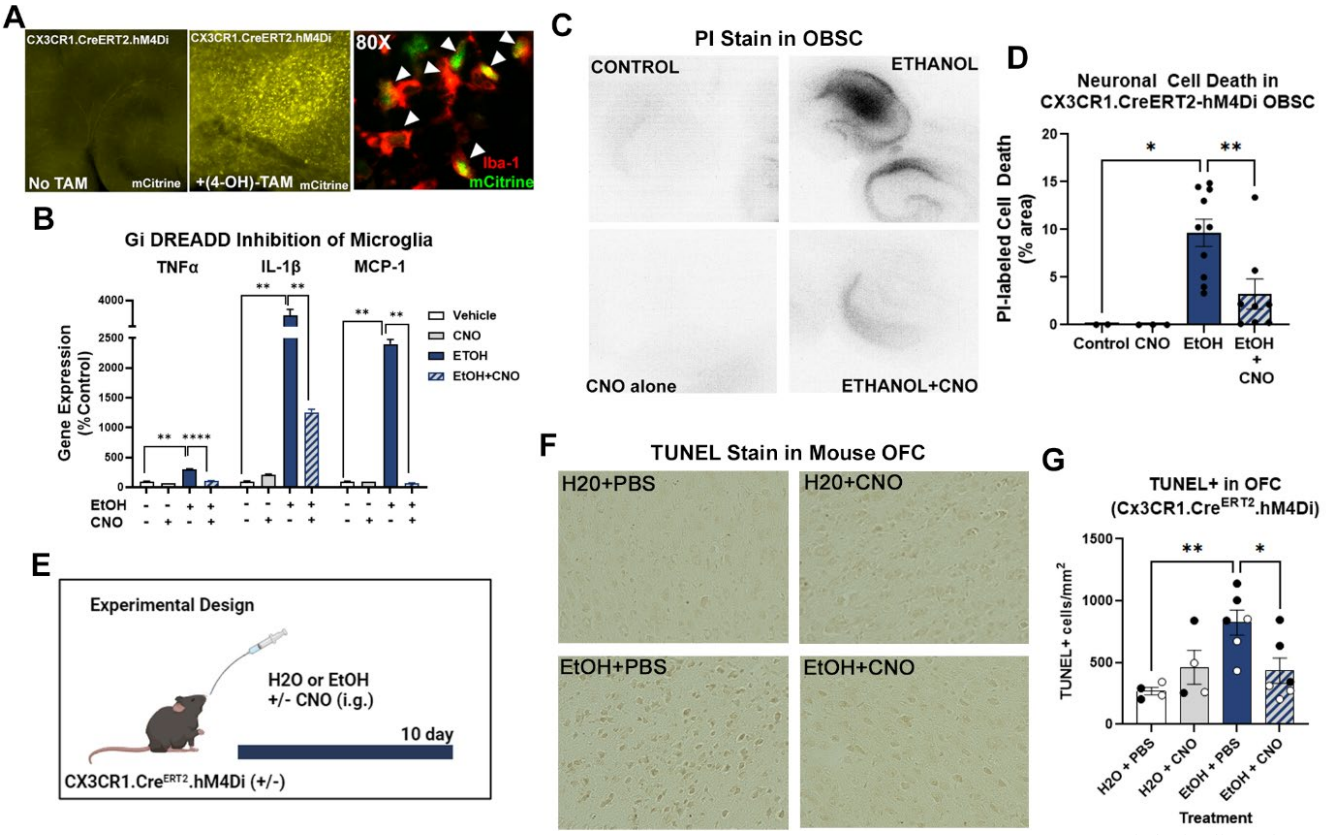

Figure 6. Gi DREADD inhibition of microglia attenuates alcohol-induced inflammation and neuronal cell death. (A-D) Organotypic brain slice cultures OBSCs from CX3CR1.Cre^{ERT2}.hM4di.mCitrine (+/-) mice were used to assess the role of microglia on proinflammatory gene expression and neuronal death *ex-vivo.* **(A)** Addition of 4-OH-TAM to induce Cre recombination caused robust increase in mCitrine levels within Iba-1+ microglia consistent with microglial DREADD expression. **(B)** Ethanol caused robust increases in the gene expression of TNFα, IL-1β, and MCP-1, which was blocked by Gi DREADD signaling induced by CNO. 1-way ANOVAs, $^{**}p<0.01$, $^{****}p<0.0001$, Sidak's post-test. **(C)** Representative images propridium iodide (PI) labeling of cell death in OBSC in response to ethanol. **(D)** Ethanol (100mM, 4 days) caused a robust increase in cell death 24 hours into withdrawal, which was significantly blocked by Gi signaling induced by CNO. 1-way ANOVA, $F_{3,19}=7.133$, $p=0.0021$, $^{*}p<0.05$, $^{**}p<0.01$, Sidak's post-test. **(E-G)** Induction of hM4Di Gi DREADD inhibition of microglia *in vivo*. **(E)** CX3CR1.Cre^{ERT2}.hM4Di (+/-) mice were treated with 10 days of control or binge ethanol (5g/kg/d, i.g.) +/- CNO (3mg/kg, i.p., 11 hours after ethanol). Assessments were performed 24 hours following the final treatment. N= 4 H2O+PBS, 4 H2O+CNO, 6 EtOH+PBS, 6 EtOH+CNO. Males-open circles, females-filled circles. **(F)** Representative images of TUNEL cell death stain in OFC. **(G)** Ethanol increased TUNEL+ cell death by ~3-fold , which was prevented by Gi DREADD inhibition of proinflammatory microglia. 1-way ANOVA, $F_{3,16}=5.353$, $p=0.0096$, $^{*}p<0.05$, $^{**}p<0.01$, Sidak's post-test.

Chemogenetic inhibition of microglia prevents hyperkatifeia during abstinence from binge ethanol.

Given the persistence of proinflammatory microglial activation and negative affective during prolonged withdrawal to binge ethanol, we assessed the impact of microglial inhibition on these hyperkatifeia phenotypes. Ten ethanol binges caused persistent increases in cortical proinflammatory gene expression in female mice after 5 weeks of abstinence with significant increases in IFNα, IFNβ, IFNAR1 and IFNAR2 (Figure 7A). These persistent increases were prevented by microglial Gi DREADD activation with CNO during binge treatment. Particularly, IFNα, IFNβ, and IFNAR1 were significantly reduced. Western blot analysis of the cortex found that cleaved, 15kD BDNF was persistently reduced with ethanol, but returned to control levels by CNO (Figure 7B-C). Behavioral testing on these mice included open field and conditioned fear memory assessments at 3 and 34

days into withdrawal and prolonged abstinence from 10 daily ethanol binges (Figure 7D). In the open field, ethanol-treated mice showed a trend toward reduced total distance traveled and spent significantly less time in the center of the open field (Figure 7E-F) consistent with findings in males above (Figure 5B). Gi DREADD microglial inhibition in females prevented this measure of anxiety-like behavior, returning center time to control (Figure 7F). Interestingly, time spent in the center was negatively correlated with IFNα and IFNβ, two genes significantly blocked by microglial inhibition (Figure 7G,H). Additionally, fine motor movement followed a similar pattern, decreasing with binge ethanol and returning to control levels with microglial inhibition (Figure 7I). In conditioned fear memory trials, ethanol persistently increased contextual fear memory during abstinence, which was prevented by microglial inhibition (Figure 7J). Similar to findings in males, 10 ethanol binges blocked the extinction of cued conditioned fear memory, with mice that received microglial inhibition during binge ethanol protected from this phenotype (Figure 7K). Similar to time spent in the center, cued fear memory extinction was negatively correlated with IFNα and IFNβ gene expression levels (Figure 7L-M).

The approach used to inhibit microglia in this model, seems to be insufficient when assessing behavior in males. As mentioned above, the CX3CR1.Cre^{ERT2} mouse causes a functional null mutation in the inserted CX3CR1 allele. In male mice, this seems to have been problematic, as the persistent proinflammatory signaling observed in WT mice (Figure 5), was not seen in male CX3CR1.Cre^{ERT2}.hm4di mice (Supplemental Figure 2A). Further, hM4Di expression in the females was more than 75% higher in females than males (Supplemental Figure 2B). In the open field, a trend toward a significant reduction in center time was found that was not affected by microglial inhibition (Supplemental Figure 2C). Further, no change was seen in contextual fear memory or extinction of cued conditioned memory in male mice receiving CNO (Supplemental Figure D-E).

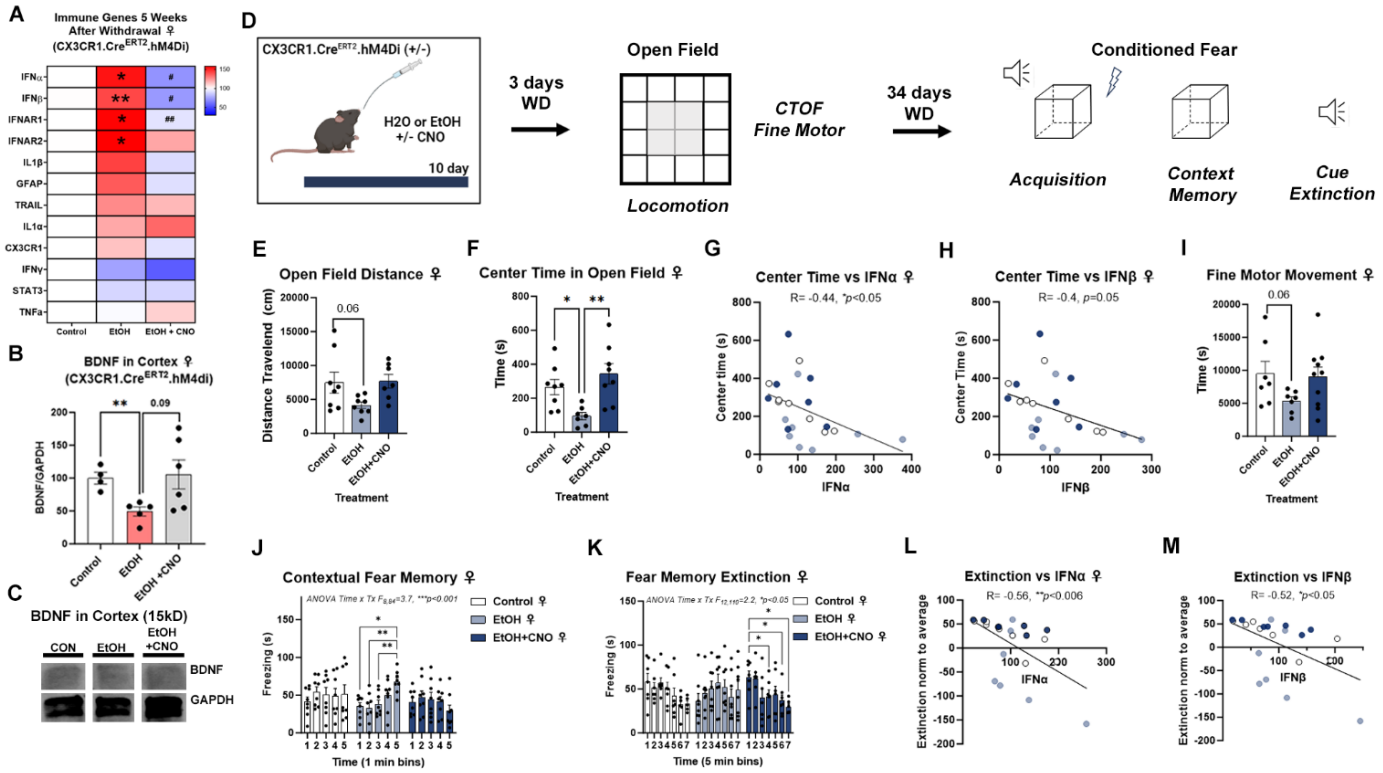

Figure 7. Gi DREADD inhibition of microglia attenuates alcohol-induced negative affect and cognitive dysfunction in females. Mice with Gi DREADD inhibition of microglia (CX3CR1.Cre^{ERT2}.hM4Di) were treated with 10 days of control or binge ethanol (5g/kg/d, i.g.) +/- CNO. (H2O+PBS=8 females, EtOH+PBS=8 females, EtOH+CNO=8 females) **(A)** Proinflammatory gene expression following 5 weeks of abstinence. Expression of inflammatory genes IFNα (*p<0.05), IFNβ (**p<0.01), IFNAR1 (*p<0.05), and IFNAR2 (*p<0.05), was significantly increased following 10-day binge ethanol. Gi DREADD inhibition of microglia significantly decreased

expression of IFNα (*p<0.05), IFNβ (*p<0.05), and IFNAR1 (**p<0.01). **(B)** Representative images and **(C)** analysis for BDNF Western blot in female cortex. Ethanol significantly decreased BDNF in the cortex (*p<0.01), which was blocked with the addition of CNO (p=0.09). **(D)** These mice underwent open field testing for anxiety-like behavior at 3 days of withdrawal and conditioned fear for acquisition and extinction at 34 days of withdrawal. **(E)** Microglial inhibition reversed the decrease in open field distance traveled (cm) seen with 10-day binge ethanol. p=0.06. **(F)** Binge ethanol increased anxiety-like behavior seen by decreased center time in open field (s), which was then returned to baseline with CNO *p<0.05, **p<0.01. **(G-H)** Time (s) spent in center of open field negatively correlated to increasing **(G)** IFNα (R=-.44, *p<0.05) and **(H)** IFNβ (R=-0.4, p=0.05) gene expression in the female cortex. **(I)** Microglial inhibition blocked the decreased fine motor movement from binge ethanol in the open field test. p=0.06. **(J)** In contextual fear memory assessments, ethanol-induced increases in freezing (s) were prevented by CNO. *p<0.05, **p<0.01 Sidak's post-test. **(K)** 10-day binge ethanol disrupted extinction of conditioned fear memory, which was restored by microglial inhibition during the ethanol binge. *p<0.05. **(L-M)** Extinction of cued conditioned fear was negatively correlated with expression of **(L)** IFNα, R= -0.56, **p<0.006 and **(M)** IFNβ, R=-0.52, *p<0.05. N= 8 H2O+PBS, 8, EtOH+PBS, and 8 EtOH+CNO.

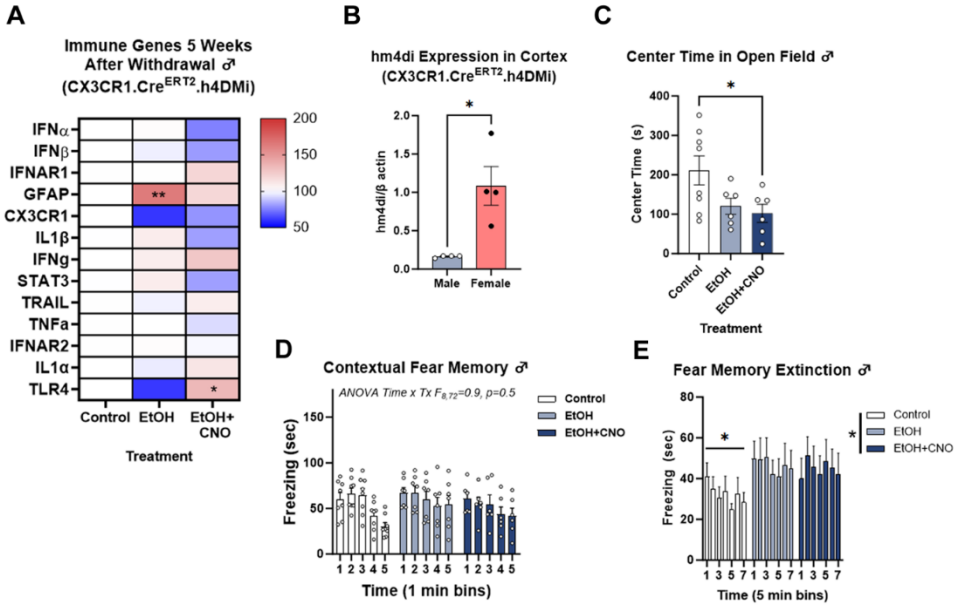

Supplemental Figure 2: Gi DREADD inhibition of microglia in males. Male mice with Gi DREADD inhibition of microglia (CX3CR1.Cre^{ERT2}.hM4Di) were treated with 10 days of control or binge ethanol (5g/kg/d, i.g.) +/- CNO. These mice underwent open field testing for anxiety-like behavior at 3 days of withdrawal and conditioned fear for acquisition and extinction at 34 days of withdrawal. **(A)** Immune gene expression at five weeks of withdrawal in males showed significantly increased GFAP with ethanol (**p<0.01) and increased TLR4 expression with the addition of CNO (*p<0.05). **(B)** RT-PCR for hM4Di expression in cortex at 5 weeks of withdrawal. Female controls had significantly increased expression of hM4Di compared to male controls. *p<0.05. **(C)** In open field testing, male mice spent significantly less center time in the open field with binge ethanol, which was also seen with the addition of CNO. *p<0.05. **(D)** No change in contextual fear memory was observed between groups in males. **(E)** Male mice treated with ethanol alone and ethanol + CNO failed to extinguish fear memory compared to the control group. *p<0.05.
(H2O+PBS: N=7 males, 8 females, EtOH+PBS: N=7 males, 8 females, EtOH+CNO: N=4 males, 8 females)

Discussion

AUD is a devastating disease with high risk of relapse and co-morbidity with depression and PTSD despite treatment. Hyperkatifeia during withdrawal likely contributes to relapse and these co-morbidities, though it is not clear what drives these anxiety-like states. Further, there are no available therapeutics that prevent or treat hyperkatifeia during withdrawal. Thus, the present work on the cellular mechanisms promoting hyperkatifeia is crucial for understanding pathways driving this negative affect state and elucidating targets for more effective treatments. Here, we found immediate and persistent proinflammatory and neuronal activation, loss of the trophic factor BDNF, and a persistent negative affective state seen during withdrawal from binge ethanol. Gi DREADD inhibition of microglia during binge ethanol prevented these effects, finding that microglia play a role in driving these alcohol-induced proinflammatory phenotypes and hyperkatifeia.

We and others have reported immediate increases in proinflammatory activation after binge ethanol, seen by induction of proinflammatory cytokines by way of the NF-kB pathway and increased gene expression[39, 61-64]. This has been thought to contribute to alcohol-induced neurodegeneration[36, 64, 65]. However, few studies have assessed proinflammatory activation during prolonged abstinence in adult mice. Our findings are consistent with a recent report finding depressive behavior and increased cytokines 5 days into withdrawal from binge ethanol

in PFC, hippocampus and striatum[66], as well as other studies assessing brain cytokines at 3 and 5 days into withdrawal[67, 68]. After adolescent binge ethanol, slight, yet persistent increases in proinflammatory cytokines are found that are enhanced in Alzheimer's disease models[69, 70]. In humans abstinent for 18 days, plasma levels of IL-8, IL1β, and IL-6 were increased, with IL-8 being correlated with craving[71]. However, we now report persistent induction of proinflammatory cytokines in cortex and microglial structural changes consistent with proinflammatory activation in stress regions at 4 and 5 weeks into prolonged abstinence. The restoration of negative affective/hyperkatifeia phenotypes with inhibition of proinflammatory microglia strongly implicates their role in these persistently detrimental phenotypes. Multiple factors may be driving these proinflammatory phenotypes. Our prior work has identified extracellular vesicles as mediators of ethanol-induced neuroinflammation and loss of hippocampal neurogenesis through epigenetic mechanisms[34, 49]. However, future studies should identify molecular mediators within microglia that could be targeted therapeutically. Of note, we have found protective phenotypes of regenerated microglia, which repopulate the brain after CSFR1-mediated microglial depletion[72, 73]. Regenerated microglia have a more trophic phenotype and less proinflammatory responses to alcohol[55, 74]. By identifying regulators of the regenerative microglial phenotype, future studies will hope to identify novel therapeutic approaches.

Several studies find a role for increased neuronal activity in affect-related regions and circuits, including hyperexcitability in the IL and BNST with ethanol[75]. Additionally, FosB has been found to be an of indicator neuronal activation in the brain, therefore we used FosB as a measure for recent (within the last 18-24h) neuronal activation[76]. With FosB staining, we found increased neuronal activation in both the IL and BSNT regions, consistent with these previous studies[77, 78]. Correlation analyses are consistent with the known circuits connecting the ventral and dorsal BNST, CeA, and IL. Circuits connecting these regions have been previously described in the setting of alcohol use as well as cannabinoids[79, 80]. Previous studies have also shown that neuronal activation in the CeA promotes alcohol self-administration drinking behavior[81]. Here, we sought to assess the associations between neuronal activity in the specific circuitry and proinflammatory activation. Neuronal activation was correlated with microglial activation in the CeA and BNST, suggesting microglia may promote increased neuronal firing with chronic binge ethanol. Future studies will directly assess the dynamic regulatory role of microglia on these circuits.

BDNF is known to be altered in AUD and related to AUD behavioral phenotypes. Previous studies have linked excessive drinking behaviors in rats with lower levels of BDNF in the BNST and amygdala[82]. Additional work found that knocking down BDNF with antisense oligonucleotides in the CeA increases anxiety-like behavior and alcohol self-administration[47]. Reductions in BDNF in human plasma have implicated the amygdala in anxiety-like behavior[83]. Our findings of reduced levels of BDNF both acutely and 4 weeks into withdrawal in the dBNST and CeA raise the question as to whether BDNF regulates neuronal activity in these regions. Indeed, a recent study found that BDNF application reduces excitability of neurons in the BNST, with BDNF/TrkB signaling needed for LTD in BNST neurons[84]. Our present findings support this idea as we observed that BDNF levels are negatively correlated with neuronal activation in the dBNST and CeA. Considering the role of BDNF in neuronal

function and negative affect, future studies should examine the specific mechanisms by which BDNF loss is associated with proinflammatory signaling and promotes hyperkatifeia.

Microglial activation is associated with alcohol-induced proinflammatory gene activation neuronal death[74, 85-87]. Recently, microglial depletion has been shown to blunt the acute proinflammatory gene activation with binge ethanol[43]. However, a causative relationship of microglia with alcohol-induced neurodegeneration has not yet been shown. Here we find that chemogenetic inhibition, which we and others have employed previously[51, 55, 74, 88], shows a similar blunting of proinflammatory gene activation with ethanol. We observed chemogenetic inhibition of microglia blocked the persistent proinflammatory gene expression, particularly IFNα and IFNβ, in the cortex at five weeks of alcohol withdrawal. Together, these previous and current data support a role for microglia in persistent ethanol-induced proinflammatory activation. However, future studies should determine if chemogenetic inhibition of microglia after binge ethanol can reverse the persistent proinflammatory activation during abstinence that we have observed. Prior studies have suggested that microglia are involved in ethanol-induced neurodegeneration through the release of extracellular vesicles[38]. For the first time, we now provide definitive evidence using Gi DREADD inhibition of microglia, which blocked ethanol-induced neuronal death. Future studies should further define these specific mechanisms to identify druggable therapeutic targets.

Lastly, we find microglia promote persistent negative-affective states during withdrawal and prolonged abstinence from alcohol. Chemogenetic microglial inhibition prevented anxiety-like and fear memory phenotypes. This is consistent with work using microglial depletion, which prevented the alcohol dependence-induced escalation of drinking and reduced sucrose intake, a measure of anhedonia[44]. However, it is not clear whether inhibiting microglia after binge alcohol-induced negative affect or dependence-induced escalation of drinking would reverse these AUD phenotypes. These are ongoing and future directions in our group. However, it is important to note that the approach using the CX3CR1 promoter was limited in its assessment of male mice. Expression of the Gi DREADD was not effectively induced in males, seen by the dramatically reduced hM4Di gene expression compared to females. Further, male CX3CR1.Cre^{ERT2}.hM4di (+/-) mice did not show persistent proinflammatory gene induction seen in male WT mice. In this model, a copy of CX3CR1, a G-coupled protein receptor with anti-inflammatory properties[89], is lost with Cre gene insertion. Males may be more sensitive to this loss than female mice. Further, we believe the loss of the CX3CR1 allele could have an impact on complex behaviors. Therefore, an alternative microglial specific promoter such as Tmem119 may be a better model for microglial inhibition to effectively elucidate mechanisms driving ethanol-induced deficits in complex behaviors. Another area of future interest involves the role of type I interferon signaling (e.g., IFNα and IFNβ), which were upregulated at five weeks of withdrawal. These genes were negatively correlated with center time (anxiety-like behavior) and fear extinction (PTSD-like behavioral inflexibility), suggesting IFN signaling might promote these behaviors. Indeed, heightened IFN signaling promotes depressive phenotypes in other settings[90-93]. Deciphering the contribution of IFN signaling to alcohol-induced hyperkatifeia is an ongoing focus in our group.

In summary, we find that chronic binge ethanol induces proinflammatory activation, loss of BDNF, neuronal cell death, and negative affect during acute withdrawal and prolonged abstinence. These outcomes were blocked by chemogenetic inhibition of proinflammatory microglia, implicating microglia as drivers of alcohol-induced

hyperkatifeia. Future work will assess specific molecular mechanisms by which microglia promotes these negative-affect states and other related AUD phenotypes.

References

(1) Whiteford, H. A.; Ferrari, A. J.; Degenhardt, L.; Feigin, V.; Vos, T. The global burden of mental, neurological and substance use disorders: an analysis from the Global Burden of Disease Study 2010. *PLoS One* **2015**, *10* (2), e0116820. DOI: 10.1371/journal.pone.0116820.

(2) Goldstein, R. B.; Chou, S. P.; Smith, S. M.; Jung, J.; Zhang, H.; Saha, T. D.; Pickering, R. P.; Ruan, W. J.; Huang, B.; Grant, B. F. Nosologic Comparisons of DSM-IV and DSM-5 Alcohol and Drug Use Disorders: Results From the National Epidemiologic Survey on Alcohol and Related Conditions-III. *J Stud Alcohol Drugs* **2015**, *76* (3), 378-388. DOI: 10.15288/jsad.2015.76.378.

(3) Burnette, E. M.; Nieto, S. J.; Grodin, E. N.; Meredith, L. R.; Hurley, B.; Miotto, K.; Gillis, A. J.; Ray, L. A. Novel Agents for the Pharmacological Treatment of Alcohol Use Disorder. *Drugs* **2022**, *82* (3), 251-274. DOI: 10.1007/s40265-021-01670-3.

(4) Anderson, P.; O'Donnell, A.; Kaner, E. Managing Alcohol Use Disorder in Primary Health Care. *Curr Psychiatry Rep* **2017**, *19* (11), 79. DOI: 10.1007/s11920-017-0837-z.

(5) Whitford, J. L.; Widner, S. C.; Mellick, D.; Elkins, R. L. Self-report of drinking compared to objective markers of alcohol consumption. *Am J Drug Alcohol Abuse* **2009**, *35* (2), 55-58. DOI: 10.1080/00952990802295212.

(6) Maisto, S. A.; Pollock, N. K.; Cornelius, J. R.; Lynch, K. G.; Martin, C. S. Alcohol relapse as a function of relapse definition in a clinical sample of adolescents. *Addict Behav* **2003**, *28* (3), 449-459. DOI: 10.1016/s0306-4603(01)00267-2.

(7) Sliedrecht, W.; de Waart, R.; Witkiewitz, K.; Roozen, H. G. Alcohol use disorder relapse factors: A systematic review. *Psychiatry Res* **2019**, *278*, 97-115. DOI: 10.1016/j.psychres.2019.05.038.

(8) Sinha, R. How does stress increase risk of drug abuse and relapse? *Psychopharmacology (Berl)* **2001**, *158* (4), 343-359. DOI: 10.1007/s002130100917.

(9) Greenfield, S. F.; Weiss, R. D.; Muenz, L. R.; Vagge, L. M.; Kelly, J. F.; Bello, L. R.; Michael, J. The effect of depression on return to drinking: a prospective study. *Arch Gen Psychiatry* **1998**, *55* (3), 259-265. DOI: 10.1001/archpsyc.55.3.259.

(10) Cooper, M. L.; Russell, M.; Skinner, J. B.; Frone, M. R.; Mudar, P. Stress and alcohol use: moderating effects of gender, coping, and alcohol expectancies. *J Abnorm Psychol* **1992**, *101* (1), 139-152. DOI: 10.1037//0021-843x.101.1.139.

(11) Brown, S. A.; Vik, P. W.; Patterson, T. L.; Grant, I.; Schuckit, M. A. Stress, vulnerability and adult alcohol relapse. *J Stud Alcohol* **1995**, *56* (5), 538-545. DOI: 10.15288/jsa.1995.56.538.

(12) Sinha, R.; Fox, H. C.; Hong, K. A.; Bergquist, K.; Bhagwagar, Z.; Siedlarz, K. M. Enhanced negative emotion and alcohol craving, and altered physiological responses following stress and cue exposure in alcohol dependent individuals. *Neuropsychopharmacology* **2009**, *34* (5), 1198-1208. DOI: 10.1038/npp.2008.78.

(13) Blanco, C.; Xu, Y.; Brady, K.; Pérez-Fuentes, G.; Okuda, M.; Wang, S. Comorbidity of posttraumatic stress disorder with alcohol dependence among US adults: results from National Epidemiological Survey on Alcohol and Related Conditions. *Drug Alcohol Depend* **2013**, *132* (3), 630-638. DOI: 10.1016/j.drugalcdep.2013.04.016.

(14) Gielen, N.; Havermans, R. C.; Tekelenburg, M.; Jansen, A. Prevalence of post-traumatic stress disorder among patients with substance use disorder: it is higher than clinicians think it is. *Eur J Psychotraumatol* **2012**, *3*. DOI: 10.3402/ejpt.v3i0.17734.

(15) Read, J. P.; Brown, P. J.; Kahler, C. W. Substance use and posttraumatic stress disorders: symptom interplay and effects on outcome. *Addict Behav* **2004**, *29* (8), 1665-1672. DOI: 10.1016/j.addbeh.2004.02.061.

(16) Keyes, K. M.; Hatzenbuehler, M. L.; Hasin, D. S. Stressful life experiences, alcohol consumption, and alcohol use disorders: the epidemiologic evidence for four main types of stressors. *Psychopharmacology* **2011**, *218* (1), 1-17. DOI: 10.1007/s00213-011-2236-1 From NLM Medline.

(17) Fetzner, M. G.; McMillan, K. A.; Sareen, J.; Asmundson, G. J. What is the association between traumatic life events and alcohol abuse/dependence in people with and without PTSD? Findings from a nationally representative sample. *Depress Anxiety* **2011**, *28* (8), 632-638. DOI: 10.1002/da.20852.

(18) Huang, M. C.; Schwandt, M. L.; Ramchandani, V. A.; George, D. T.; Heilig, M. Impact of multiple types of childhood trauma exposure on risk of psychiatric comorbidity among alcoholic inpatients. *Alcohol Clin Exp Res* **2012**, *36* (6), 1099-1107. DOI: 10.1111/j.1530-0277.2011.01695.x.

(19) Elsayed, N. M.; Kim, M. J.; Fields, K. M.; Olvera, R. L.; Hariri, A. R.; Williamson, D. E. Trajectories of Alcohol Initiation and Use During Adolescence: The Role of Stress and Amygdala Reactivity. *J Am Acad Child Adolesc Psychiatry* **2018**, *57* (8), 550-560. DOI: 10.1016/j.jaac.2018.05.011.
(20) Lê, A. D.; Quan, B.; Juzytch, W.; Fletcher, P. J.; Joharchi, N.; Shaham, Y. Reinstatement of alcohol-seeking by priming injections of alcohol and exposure to stress in rats. *Psychopharmacology (Berl)* **1998**, *135* (2), 169-174. DOI: 10.1007/s002130050498.
(21) Breese, G. R.; Overstreet, D. H.; Knapp, D. J. Conceptual framework for the etiology of alcoholism: a "kindling"/stress hypothesis. *Psychopharmacology (Berl)* **2005**, *178* (4), 367-380. DOI: 10.1007/s00213-004-2016-2.
(22) Marcinkiewcz, C. A.; Dorrier, C. E.; Lopez, A. J.; Kash, T. L. Ethanol induced adaptations in 5-HT2c receptor signaling in the bed nucleus of the stria terminalis: implications for anxiety during ethanol withdrawal. *Neuropharmacology* **2015**, *89*, 157-167. DOI: 10.1016/j.neuropharm.2014.09.003.
(23) Delfs, J. M.; Zhu, Y.; Druhan, J. P.; Aston-Jones, G. Noradrenaline in the ventral forebrain is critical for opiate withdrawal-induced aversion. *Nature* **2000**, *403* (6768), 430-434. DOI: 10.1038/35000212.
(24) Pati, D.; Marcinkiewcz, C. A.; DiBerto, J. F.; Cogan, E. S.; McElligott, Z. A.; Kash, T. L. Chronic intermittent ethanol exposure dysregulates a GABAergic microcircuit in the bed nucleus of the stria terminalis. *Neuropharmacology* **2020**, *168*, 107759. DOI: 10.1016/j.neuropharm.2019.107759.
(25) Sink, K. S.; Walker, D. L.; Freeman, S. M.; Flandreau, E. I.; Ressler, K. J.; Davis, M. Effects of continuously enhanced corticotropin releasing factor expression within the bed nucleus of the stria terminalis on conditioned and unconditioned anxiety. *Mol Psychiatry* **2013**, *18* (3), 308-319. DOI: 10.1038/mp.2011.188.
(26) Walker, D. L.; Toufexis, D. J.; Davis, M. Role of the bed nucleus of the stria terminalis versus the amygdala in fear, stress, and anxiety. *Eur J Pharmacol* **2003**, *463* (1-3), 199-216. DOI: 10.1016/s0014-2999(03)01282-2.
(27) LaBar, K. S.; Gatenby, J. C.; Gore, J. C.; LeDoux, J. E.; Phelps, E. A. Human amygdala activation during conditioned fear acquisition and extinction: a mixed-trial fMRI study. *Neuron* **1998**, *20* (5), 937-945. DOI: 10.1016/s0896-6273(00)80475-4.
(28) Flores-Ramirez, F. J.; Varodayan, F. P.; Patel, R. R.; Illenberger, J. M.; Di Ottavio, F.; Roberto, M.; Martin-Fardon, R. Blockade of orexin receptors in the infralimbic cortex prevents stress-induced reinstatement of alcohol-seeking behaviour in alcohol-dependent rats. *Br J Pharmacol* **2023**, *180* (11), 1500-1515. DOI: 10.1111/bph.16015.
(29) Flores-Ramirez, F. J.; Matzeu, A.; Sánchez-Marín, L.; Martin-Fardon, R. Blockade of corticotropin-releasing factor-1 receptors in the infralimbic cortex prevents stress-induced reinstatement of alcohol seeking in male Wistar rats: Evidence of interaction between CRF. *Neuropharmacology* **2022**, *210*, 109046. DOI: 10.1016/j.neuropharm.2022.109046.
(30) Yu, Y.; Yuan, Z.; Fan, Y.; Li, J.; Wu, Y. Dynamic Transitions in Neuronal Network Firing Sustained by Abnormal Astrocyte Feedback. *Neural Plast* **2020**, *2020*, 8864246. DOI: 10.1155/2020/8864246.
(31) Wang, C.; Yue, H.; Hu, Z.; Shen, Y.; Ma, J.; Li, J.; Wang, X. D.; Wang, L.; Sun, B.; Shi, P.; et al. Microglia mediate forgetting via complement-dependent synaptic elimination. *Science* **2020**, *367* (6478), 688-694. DOI: 10.1126/science.aaz2288.
(32) Lan, L.; Wang, H.; Zhang, X.; Shen, Q.; Li, X.; He, L.; Rong, X.; Peng, J.; Mo, J.; Peng, Y. Chronic exposure of alcohol triggers microglia-mediated synaptic elimination inducing cognitive impairment. *Exp Neurol* **2022**, *353*, 114061. DOI: 10.1016/j.expneurol.2022.114061.
(33) Peng, H.; Geil Nickell, C. R.; Chen, K. Y.; McClain, J. A.; Nixon, K. Increased expression of M1 and M2 phenotypic markers in isolated microglia after four-day binge alcohol exposure in male rats. *Alcohol* **2017**, *62*, 29-40. DOI: 10.1016/j.alcohol.2017.02.175.
(34) Crews, F. T.; Zou, J.; Coleman, L. G. Extracellular microvesicles promote microglia-mediated pro-inflammatory responses to ethanol. *J Neurosci Res* **2021**, *99* (8), 1940-1956. DOI: 10.1002/jnr.24813.
(35) Walter, T. J.; Crews, F. T. Microglial depletion alters the brain neuroimmune response to acute binge ethanol withdrawal. *J Neuroinflammation* **2017**, *14* (1), 86. DOI: 10.1186/s12974-017-0856-z.
(36) Zou, J.; Crews, F. Induction of innate immune gene expression cascades in brain slice cultures by ethanol: key role of NF-κB and proinflammatory cytokines. *Alcohol Clin Exp Res* **2010**, *34* (5), 777-789. DOI: 10.1111/j.1530-0277.2010.01150.x.
(37) Vetreno, R. P.; Qin, L.; Coleman, L. G., Jr.; Crews, F. T. Increased Toll-like Receptor-MyD88-NFkappaB-Proinflammatory neuroimmune signaling in the orbitofrontal cortex of humans with alcohol use disorder. *Alcoholism, clinical and experimental research* **2021**, *45* (9), 1747-1761. DOI: 10.1111/acer.14669 From NLM Medline.

(38) Coleman, L. G., Jr.; Zou, J.; Crews, F. T. Microglial-derived miRNA let-7 and HMGB1 contribute to ethanol-induced neurotoxicity via TLR7. *Journal of neuroinflammation* **2017**, *14* (1), 22. DOI: 10.1186/s12974-017-0799-4.
(39) Crews, F. T.; Qin, L.; Sheedy, D.; Vetreno, R. P.; Zou, J. High mobility group box 1/Toll-like receptor danger signaling increases brain neuroimmune activation in alcohol dependence. *Biological psychiatry* **2013**, *73* (7), 602-612. DOI: 10.1016/j.biopsych.2012.09.030.
(40) Qin, L.; Zou, J.; Barnett, A.; Vetreno, R. P.; Crews, F. T.; Coleman, L. G. TRAIL Mediates Neuronal Death in AUD: A Link between Neuroinflammation and Neurodegeneration. *International journal of molecular sciences* **2021**, *22* (5), 2547.
(41) Lovelock, D. F.; Liu, W.; Langston, S. E.; Liu, J.; Van Voorhies, K.; Giffin, K. A.; Vetreno, R. P.; Crews, F. T.; Besheer, J. The Toll-like receptor 7 agonist imiquimod increases ethanol self-administration and induces expression of Toll-like receptor related genes. *Addict Biol* **2022**, *27* (3), e13176. DOI: 10.1111/adb.13176.
(42) Lovelock, D. F.; Randall, P. A.; Van Voorhies, K.; Vetreno, R. P.; Crews, F. T.; Besheer, J. Increased alcohol self-administration following repeated Toll-like receptor 3 agonist treatment in male and female rats. *Pharmacol Biochem Behav* **2022**, *216*, 173379. DOI: 10.1016/j.pbb.2022.173379.
(43) Warden, A. S.; Wolfe, S. A.; Khom, S.; Varodayan, F. P.; Patel, R. R.; Steinman, M. Q.; Bajo, M.; Montgomery, S. E.; Vlkolinsky, R.; Nadav, T.; et al. Microglia Control Escalation of Drinking in Alcohol-Dependent Mice: Genomic and Synaptic Drivers. *Biol Psychiatry* **2020**, *88* (12), 910-921. DOI: 10.1016/j.biopsych.2020.05.011.
(44) Warden, A. S.; Triplett, T. A.; Lyu, A.; Grantham, E. K.; Azzam, M. M.; DaCosta, A.; Mason, S.; Blednov, Y. A.; Ehrlich, L. I. R.; Mayfield, R. D.; et al. Microglia depletion and alcohol: Transcriptome and behavioral profiles. *Addict Biol* **2021**, *26* (2), e12889. DOI: 10.1111/adb.12889.
(45) Breese, G. R.; Knapp, D. J.; Overstreet, D. H.; Navarro, M.; Wills, T. A.; Angel, R. A. Repeated lipopolysaccharide (LPS) or cytokine treatments sensitize ethanol withdrawal-induced anxiety-like behavior. *Neuropsychopharmacology* **2008**, *33* (4), 867-876. DOI: 10.1038/sj.npp.1301468.
(46) Duivis, H. E.; Vogelzangs, N.; Kupper, N.; de Jonge, P.; Penninx, B. W. Differential association of somatic and cognitive symptoms of depression and anxiety with inflammation: findings from the Netherlands Study of Depression and Anxiety (NESDA). *Psychoneuroendocrinology* **2013**, *38* (9), 1573-1585. DOI: 10.1016/j.psyneuen.2013.01.002.
(47) Pandey, S. C.; Zhang, H.; Roy, A.; Misra, K. Central and medial amygdaloid brain-derived neurotrophic factor signaling plays a critical role in alcohol-drinking and anxiety-like behaviors. *J Neurosci* **2006**, *26* (32), 8320-8331. DOI: 10.1523/JNEUROSCI.4988-05.2006.
(48) Silva-Peña, D.; García-Marchena, N.; Alén, F.; Araos, P.; Rivera, P.; Vargas, A.; García-Fernández, M. I.; Martín-Velasco, A. I.; Villanúa, M.; Castilla-Ortega, E.; et al. Alcohol-induced cognitive deficits are associated with decreased circulating levels of the neurotrophin BDNF in humans and rats. *Addict Biol* **2019**, *24* (5), 1019-1033. DOI: 10.1111/adb.12668.
(49) Zou, J.; Walter, T. J.; Barnett, A.; Rohlman, A.; Crews, F. T.; Coleman, L. G. Ethanol Induces Secretion of Proinflammatory Extracellular Vesicles That Inhibit Adult Hippocampal Neurogenesis Through G9a/GLP-Epigenetic Signaling. *Front Immunol* **2022**, *13*, 866073. DOI: 10.3389/fimmu.2022.866073.
(50) Zou, J.; McNair, E.; DeCastro, S.; Lyons, S. P.; Mordant, A.; Herring, L. E.; Vetreno, R. P.; Coleman, L. G. Microglia either promote or restrain TRAIL-mediated excitotoxicity caused by Aβ. *J Neuroinflammation* **2024**, *21* (1), 215. DOI: 10.1186/s12974-024-03208-2.
(51) Grace, P. M.; Wang, X.; Strand, K. A.; Baratta, M. V.; Zhang, Y.; Galer, E. L.; Yin, H.; Maier, S. F.; Watkins, L. R. DREADDed microglia in pain: Implications for spinal inflammatory signaling in male rats. *Experimental neurology* **2018**, *304*, 125-131. DOI: 10.1016/j.expneurol.2018.03.005.
(52) Bertola, A.; Mathews, S.; Ki, S. H.; Wang, H.; Gao, B. Mouse model of chronic and binge ethanol feeding (the NIAAA model). *Nature protocols* **2013**, *8* (3), 627-637. DOI: 10.1038/nprot.2013.032.
(53) Pruett, S.; Tan, W.; Howell, G. E., 3rd; Nanduri, B. Dosage scaling of alcohol in binge exposure models in mice: An empirical assessment of the relationship between dose, alcohol exposure, and peak blood concentrations in humans and mice. *Alcohol* **2020**, *89*, 9-17. DOI: 10.1016/j.alcohol.2020.03.011 From NLM Medline.
(54) Barnett, A. G.; Dawkins, L.; Zou, J.; McNair, E.; Nikolova, V.; Moy, S. G.; Sutherland, G.; Stevens, J.; Collie, M.; Katemboh, K.; et al. Loss of neuronal lysosomal acid lipase drives amyloid pathology in Alzheimer's disease. *bioRxiv* **2024**, 2024.2006.2009.596693. DOI: 10.1101/2024.06.09.596693.
(55) Zou, J.; McNair, E.; DeCastro, S.; Lyons, S. P.; Mordant, A.; Herring, L. E.; Vetreno, R. P.; Coleman, L. G., Jr. Microglia either promote or restrain TRAIL-mediated excitotoxicity caused by Abeta(1-42) oligomers. *Journal of neuroinflammation* **2024**, *21* (1), 215. DOI: 10.1186/s12974-024-03208-2 From NLM Medline.

(56) Zou, J.; Walter, T. J.; Barnett, A.; Rohlman, A.; Crews, F. T.; Coleman, L. G. Ethanol Induces Secretion of Proinflammatory Extracellular Vesicles That Inhibit Adult Hippocampal Neurogenesis Through G9a/GLP-Epigenetic Signaling. *Frontiers in immunology* **2022**, *13*, Original Research. DOI: 10.3389/fimmu.2022.866073.
(57) Barnett, A.; David, E.; Rohlman, A.; Nikolova, V. D.; Moy, S. S.; Vetreno, R. P.; Coleman, L. G. Adolescent Binge Alcohol Enhances Early Alzheimer's Disease Pathology in Adulthood Through Proinflammatory Neuroimmune Activation. *Front Pharmacol* **2022**, *13*, 884170. DOI: 10.3389/fphar.2022.884170.
(58) Qin, L.; Zou, J.; Barnett, A.; Vetreno, R. P.; Crews, F. T.; Coleman, L. G. TRAIL Mediates Neuronal Death in AUD: A Link between Neuroinflammation and Neurodegeneration. *Int J Mol Sci* **2021**, *22* (5). DOI: 10.3390/ijms22052547.
(59) Läck, A. K.; Diaz, M. R.; Chappell, A.; DuBois, D. W.; McCool, B. A. Chronic ethanol and withdrawal differentially modulate pre- and postsynaptic function at glutamatergic synapses in rat basolateral amygdala. *J Neurophysiol* **2007**, *98* (6), 3185-3196. DOI: 10.1152/jn.00189.2007.
(60) Lee, Y. B.; Nagai, A.; Kim, S. U. Cytokines, chemokines, and cytokine receptors in human microglia. *J Neurosci Res* **2002**, *69* (1), 94-103. DOI: 10.1002/jnr.10253.
(61) He, J.; Crews, F. T. Increased MCP-1 and microglia in various regions of the human alcoholic brain. *Experimental neurology* **2008**, *210* (2), 349-358. DOI: 10.1016/j.expneurol.2007.11.017.
(62) Coleman, L. G., Jr.; Crews, F. T. Innate Immune Signaling and Alcohol Use Disorders. *Handbook of experimental pharmacology* **2018**, *248*. DOI: 10.1007/164_2018_92.
(63) Coleman, L. G., Jr.; Zou, J.; Qin, L.; Crews, F. T. HMGB1/IL-1beta complexes regulate neuroimmune responses in alcoholism. *Brain, behavior, and immunity* **2018**, *72*, 61-77. DOI: 10.1016/j.bbi.2017.10.027.
(64) Alfonso-Loeches, S.; Pascual-Lucas, M.; Blanco, A. M.; Sanchez-Vera, I.; Guerri, C. Pivotal role of TLR4 receptors in alcohol-induced neuroinflammation and brain damage. *The Journal of neuroscience : the official journal of the Society for Neuroscience* **2010**, *30* (24), 8285-8295. DOI: 10.1523/JNEUROSCI.0976-10.2010.
(65) Marshall, S. A.; Geil, C. R.; Nixon, K. Prior Binge Ethanol Exposure Potentiates the Microglial Response in a Model of Alcohol-Induced Neurodegeneration. *Brain Sci* **2016**, *6* (2). DOI: 10.3390/brainsci6020016.
(66) Fraga-Junior, E. B.; Fernandes, I. L.; Rohden, C. A. H.; Doneda, D. L.; Ynoue, H. N.; Rios-Santos, F.; Lima, E.; Buss, Z. S.; Vandresen-Filho, S. Attenuation of the levels of pro-inflammatory cytokines prevents depressive-like behavior during ethanol withdrawal in mice. *Brain research bulletin* **2022**, *191*, 9-19. DOI: 10.1016/j.brainresbull.2022.10.014 From NLM Medline.
(67) Qin, L.; Crews, F. T. Chronic ethanol increases systemic TLR3 agonist-induced neuroinflammation and neurodegeneration. *Journal of neuroinflammation* **2012**, *9*, 130. DOI: 10.1186/1742-2094-9-130.
(68) Schneider, R., Jr.; Bandiera, S.; Souza, D. G.; Bellaver, B.; Caletti, G.; Quincozes-Santos, A.; Elisabetsky, E.; Gomez, R. N-acetylcysteine Prevents Alcohol Related Neuroinflammation in Rats. *Neurochemical research* **2017**, *42* (8), 2135-2141. DOI: 10.1007/s11064-017-2218-8 From NLM Medline.
(69) Vetreno, R. P.; Lawrimore, C. J.; Rowsey, P. J.; Crews, F. T. Persistent Adult Neuroimmune Activation and Loss of Hippocampal Neurogenesis Following Adolescent Ethanol Exposure: Blockade by Exercise and the Anti-inflammatory Drug Indomethacin. *Front Neurosci* **2018**, *12*, 200. DOI: 10.3389/fnins.2018.00200.
(70) Barnett, A. M.; David, E.; Rohlman, A. R.; Nikolova, V. D.; Moy, S. S.; Vetreno, R.; Coleman, L. G. Adolescent Binge Alcohol Enhances Early Alzheimer's Disease Pathology in Adulthood Through Proinflammatory Neuroimmune Activation. *Frontiers in pharmacology* **2022**, *13*, 884170, Original Research. DOI: 10.3389/fphar.2022.884170 From NLM PubMed-not-MEDLINE.
(71) Leclercq, S.; De Saeger, C.; Delzenne, N.; de Timary, P.; Starkel, P. Role of inflammatory pathways, blood mononuclear cells, and gut-derived bacterial products in alcohol dependence. *Biological psychiatry* **2014**, *76* (9), 725-733. DOI: 10.1016/j.biopsych.2014.02.003.
(72) Elmore, M. R.; Najafi, A. R.; Koike, M. A.; Dagher, N. N.; Spangenberg, E. E.; Rice, R. A.; Kitazawa, M.; Matusow, B.; Nguyen, H.; West, B. L.; et al. Colony-stimulating factor 1 receptor signaling is necessary for microglia viability, unmasking a microglia progenitor cell in the adult brain. *Neuron* **2014**, *82* (2), 380-397. DOI: 10.1016/j.neuron.2014.02.040.
(73) Hughes, E. G.; Bergles, D. E. Hidden progenitors replace microglia in the adult brain. *Neuron* **2014**, *82* (2), 253-255. DOI: 10.1016/j.neuron.2014.04.010.
(74) Coleman, L. G.; Zou, J.; Crews, F. T. Microglial depletion and repopulation in brain slice culture normalizes sensitized proinflammatory signaling. *J Neuroinflammation* **2020**, *17* (1), 27. DOI: 10.1186/s12974-019-1678-y.
(75) Pleil, K. E.; Lowery-Gionta, E. G.; Crowley, N. A.; Li, C.; Marcinkiewcz, C. A.; Rose, J. H.; McCall, N. M.; Maldonado-Devincci, A. M.; Morrow, A. L.; Jones, S. R.; et al. Effects of chronic ethanol exposure on neuronal function in the prefrontal cortex and extended amygdala. *Neuropharmacology* **2015**, *99*, 735-749. DOI: 10.1016/j.neuropharm.2015.06.017.

(76) Alibhai, I. N.; Green, T. A.; Potashkin, J. A.; Nestler, E. J. Regulation of fosB and DeltafosB mRNA expression: in vivo and in vitro studies. *Brain Res* **2007**, *1143*, 22-33. DOI: 10.1016/j.brainres.2007.01.069.
(77) Pati, D.; Downs, A. M.; McElligott, Z. A.; Kash, T. L. Chronic Ethanol Exposure Modulates Periaqueductal Gray to Extended Amygdala Dopamine Circuit. *The Journal of neuroscience : the official journal of the Society for Neuroscience* **2023**, *43* (5), 709-721. DOI: 10.1523/JNEUROSCI.1219-22.2022 From NLM Medline.
(78) Kash, T. L.; Baucum, A. J., 2nd; Conrad, K. L.; Colbran, R. J.; Winder, D. G. Alcohol exposure alters NMDAR function in the bed nucleus of the stria terminalis. *Neuropsychopharmacology : official publication of the American College of Neuropsychopharmacology* **2009**, *34* (11), 2420-2429. DOI: 10.1038/npp.2009.69 From NLM Medline.
(79) Massi, L.; Elezgarai, I.; Puente, N.; Reguero, L.; Grandes, P.; Manzoni, O. J.; Georges, F. Cannabinoid receptors in the bed nucleus of the stria terminalis control cortical excitation of midbrain dopamine cells in vivo. *J Neurosci* **2008**, *28* (42), 10496-10508. DOI: 10.1523/JNEUROSCI.2291-08.2008.
(80) Roland, A. V.; Harry Chao, T. H.; Hon, O. J.; Machinski, S. N.; Sides, T. R.; Lee, S. I.; Ian Shih, Y. Y.; Kash, T. L. Acute and chronic alcohol modulation of extended amygdala calcium dynamics. *Alcohol* **2024**, *116*, 53-64. DOI: 10.1016/j.alcohol.2024.02.004 From NLM Medline.
(81) de Guglielmo, G.; Crawford, E.; Kim, S.; Vendruscolo, L. F.; Hope, B. T.; Brennan, M.; Cole, M.; Koob, G. F.; George, O. Recruitment of a Neuronal Ensemble in the Central Nucleus of the Amygdala Is Required for Alcohol Dependence. *J Neurosci* **2016**, *36* (36), 9446-9453. DOI: 10.1523/JNEUROSCI.1395-16.2016.
(82) Prakash, A.; Zhang, H.; Pandey, S. C. Innate differences in the expression of brain-derived neurotrophic factor in the regions within the extended amygdala between alcohol preferring and nonpreferring rats. *Alcohol Clin Exp Res* **2008**, *32* (6), 909-920. DOI: 10.1111/j.1530-0277.2008.00650.x.
(83) Gorka, S. M.; Teppen, T.; Radoman, M.; Phan, K. L.; Pandey, S. C. Human Plasma BDNF Is Associated With Amygdala-Prefrontal Cortex Functional Connectivity and Problem Drinking Behaviors. *Int J Neuropsychopharmacol* **2020**, *23* (1), 1-11. DOI: 10.1093/ijnp/pyz057.
(84) Fiedler, D.; Sasi, M.; Blum, R.; Klinke, C. M.; Andreatta, M.; Pape, H. C.; Lange, M. D. Brain-Derived Neurotrophic Factor/Tropomyosin Receptor Kinase B Signaling Controls Excitability and Long-Term Depression in Oval Nucleus of the BNST. *J Neurosci* **2021**, *41* (3), 435-445. DOI: 10.1523/JNEUROSCI.1104-20.2020.
(85) Zhao, Y. N.; Wang, F.; Fan, Y. X.; Ping, G. F.; Yang, J. Y.; Wu, C. F. Activated microglia are implicated in cognitive deficits, neuronal death, and successful recovery following intermittent ethanol exposure. *Behav Brain Res* **2013**, *236* (1), 270-282. DOI: 10.1016/j.bbr.2012.08.052.
(86) Fernandez-Lizarbe, S.; Pascual, M.; Guerri, C. Critical role of TLR4 response in the activation of microglia induced by ethanol. *J Immunol* **2009**, *183* (7), 4733-4744. DOI: 10.4049/jimmunol.0803590.
(87) Fernandez-Lizarbe, S.; Montesinos, J.; Guerri, C. Ethanol induces TLR4/TLR2 association, triggering an inflammatory response in microglial cells. *J Neurochem* **2013**, *126* (2), 261-273. DOI: 10.1111/jnc.12276.
(88) Parusel, S.; Yi, M. H.; Hunt, C. L.; Wu, L. J. Chemogenetic and Optogenetic Manipulations of Microglia in Chronic Pain. *Neuroscience bulletin* **2023**, *39* (3), 368-378. DOI: 10.1007/s12264-022-00937-3 From NLM Medline.
(89) Hsiao, C. C.; Sankowski, R.; Prinz, M.; Smolders, J.; Huitinga, I.; Hamann, J. GPCRomics of Homeostatic and Disease-Associated Human Microglia. *Front Immunol* **2021**, *12*, 674189. DOI: 10.3389/fimmu.2021.674189.
(90) Callaghan, C. K.; Rouine, J.; Dean, R. L.; Knapp, B. I.; Bidlack, J. M.; Deaver, D. R.; O'Mara, S. M. Antidepressant-like effects of 3-carboxamido seco-nalmefene (3CS-nalmefene), a novel opioid receptor modulator, in a rat IFN-alpha-induced depression model. *Brain, behavior, and immunity* **2018**, *67*, 152-162. DOI: 10.1016/j.bbi.2017.08.016.
(91) Li, J.; Huang, S.; Huang, W.; Wang, W.; Wen, G.; Gao, L.; Fu, X.; Wang, M.; Liang, W.; Kwan, H. Y.; et al. Paeoniflorin ameliorates interferon-alpha-induced neuroinflammation and depressive-like behaviors in mice. *Oncotarget* **2017**, *8* (5), 8264-8282. DOI: 10.18632/oncotarget.14160.
(92) Borsini, A.; Cattaneo, A.; Malpighi, C.; Thuret, S.; Harrison, N. A.; Consortium, M. R. C. I.; Zunszain, P. A.; Pariante, C. M. Interferon-Alpha Reduces Human Hippocampal Neurogenesis and Increases Apoptosis via Activation of Distinct STAT1-Dependent Mechanisms. *The international journal of neuropsychopharmacology* **2017**. DOI: 10.1093/ijnp/pyx083.
(93) Zheng, L. S.; Kaneko, N.; Sawamoto, K. Minocycline treatment ameliorates interferon-alpha- induced neurogenic defects and depression-like behaviors in mice. *Frontiers in cellular neuroscience* **2015**, *9*, 5. DOI: 10.3389/fncel.2015.00005.

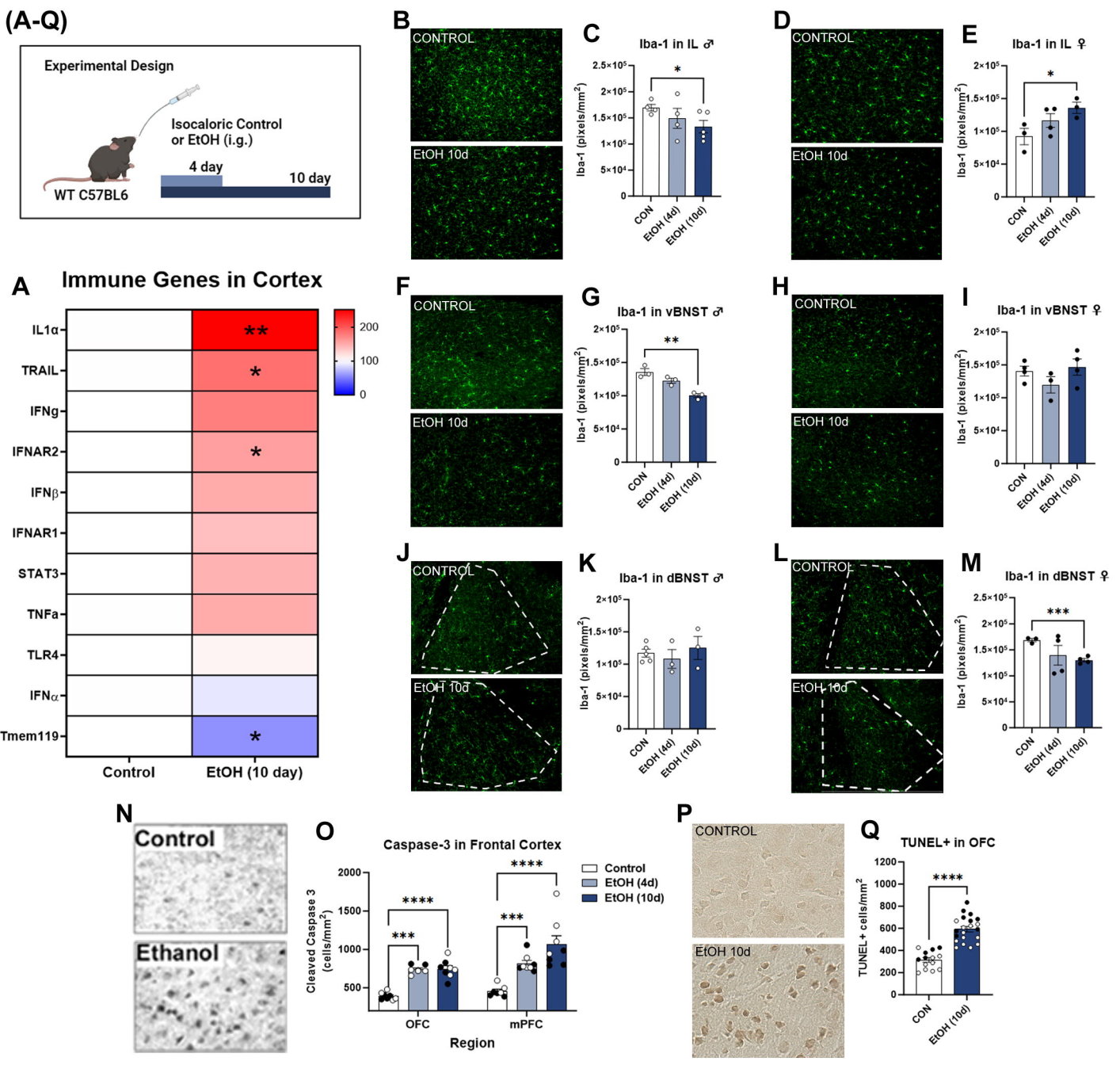
(A-Q)
Experimental Design
Isocaloric Control or EtOH (i.g.)
4 day
10 day
WT C57BL6
A
Immune Genes in Cortex
IL1α
TRAIL
IFNg
IFNAR2
IFNβ
IFNAR1
STAT3
TNFa
TLR4
IFNα
Tmem119
Control
EtOH (10 day)
B
CONTROL
EtOH 10d
C
Iba-1 in IL ♂
D
E
Iba-1 in IL ♀
F
Iba-1 in vBNST ♂
G
H
Iba-1 in vBNST ♀
I
J
Iba-1 in dBNST ♂
K
L
Iba-1 in dBNST ♀
M
Iba-1 (pixels/mm²)
CON
EtOH (4d)
EtOH (10d)
N
Control
Ethanol
O
Caspase-3 in Frontal Cortex
Cleaved Caspase 3 (cells/mm²)
OFC
mPFC
Region
P
Q
TUNEL+ in OFC
TUNEL+ cells/mm²

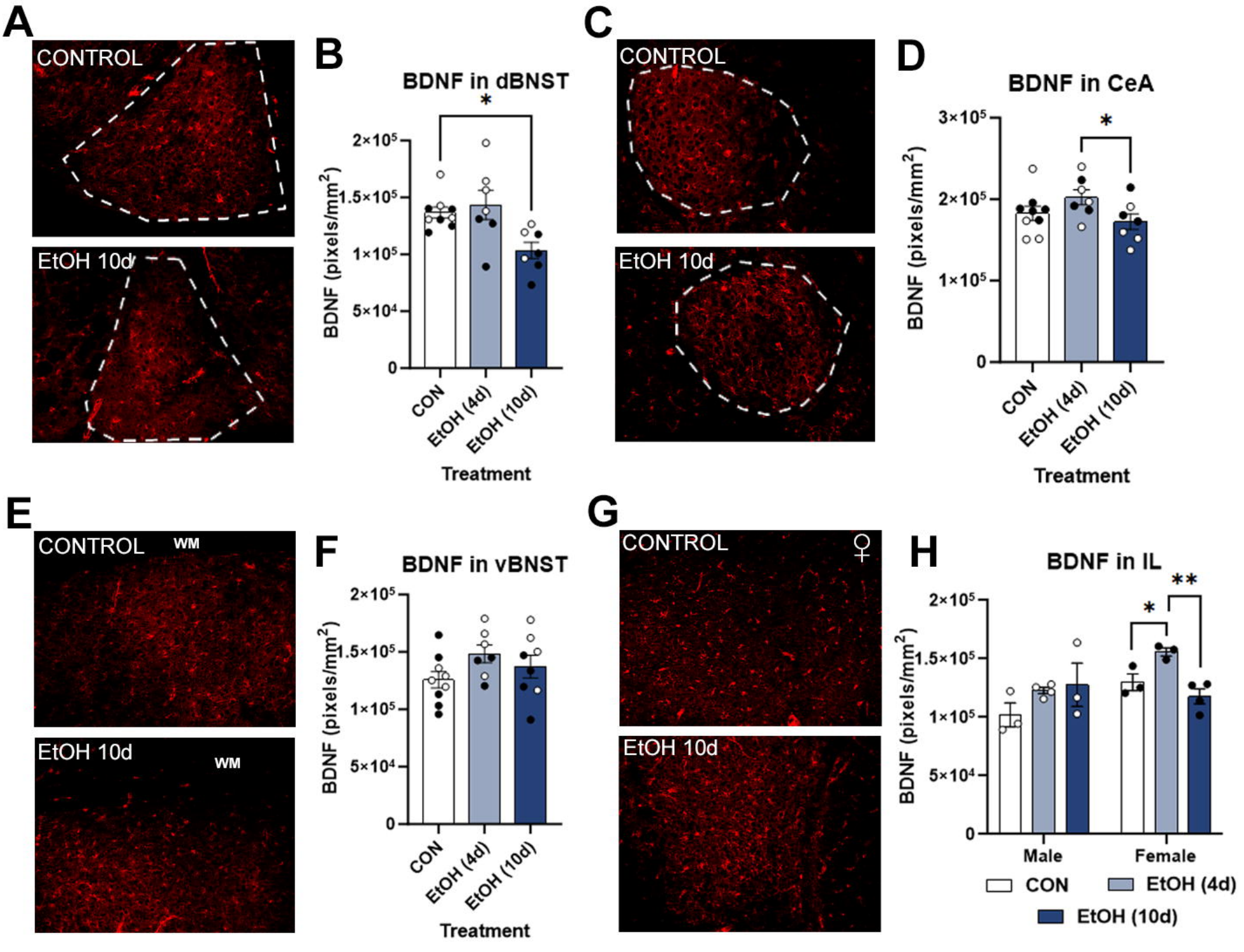
A
CONTROL
EtOH 10d
B
BDNF in dBNST
*
BDNF (pixels/mm²)
2×10⁵
1.5×10⁵
1×10⁵
5×10⁴
0
CON
EtOH (4d)
EtOH (10d)
Treatment
C
CONTROL
EtOH 10d
D
BDNF in CeA
*
BDNF (pixels/mm²)
3×10⁵
2×10⁵
1×10⁵
0
CON
EtOH (4d)
EtOH (10d)
Treatment
E
CONTROL
WM
EtOH 10d
WM
F
BDNF in vBNST
BDNF (pixels/mm²)
2×10⁵
1.5×10⁵
1×10⁵
5×10⁴
0
CON
EtOH (4d)
EtOH (10d)
Treatment
G
CONTROL
♀
EtOH 10d
H
BDNF in IL
*
**
BDNF (pixels/mm²)
2×10⁵
1.5×10⁵
1×10⁵
5×10⁴
0
Male
Female
CON
EtOH (4d)
EtOH (10d)

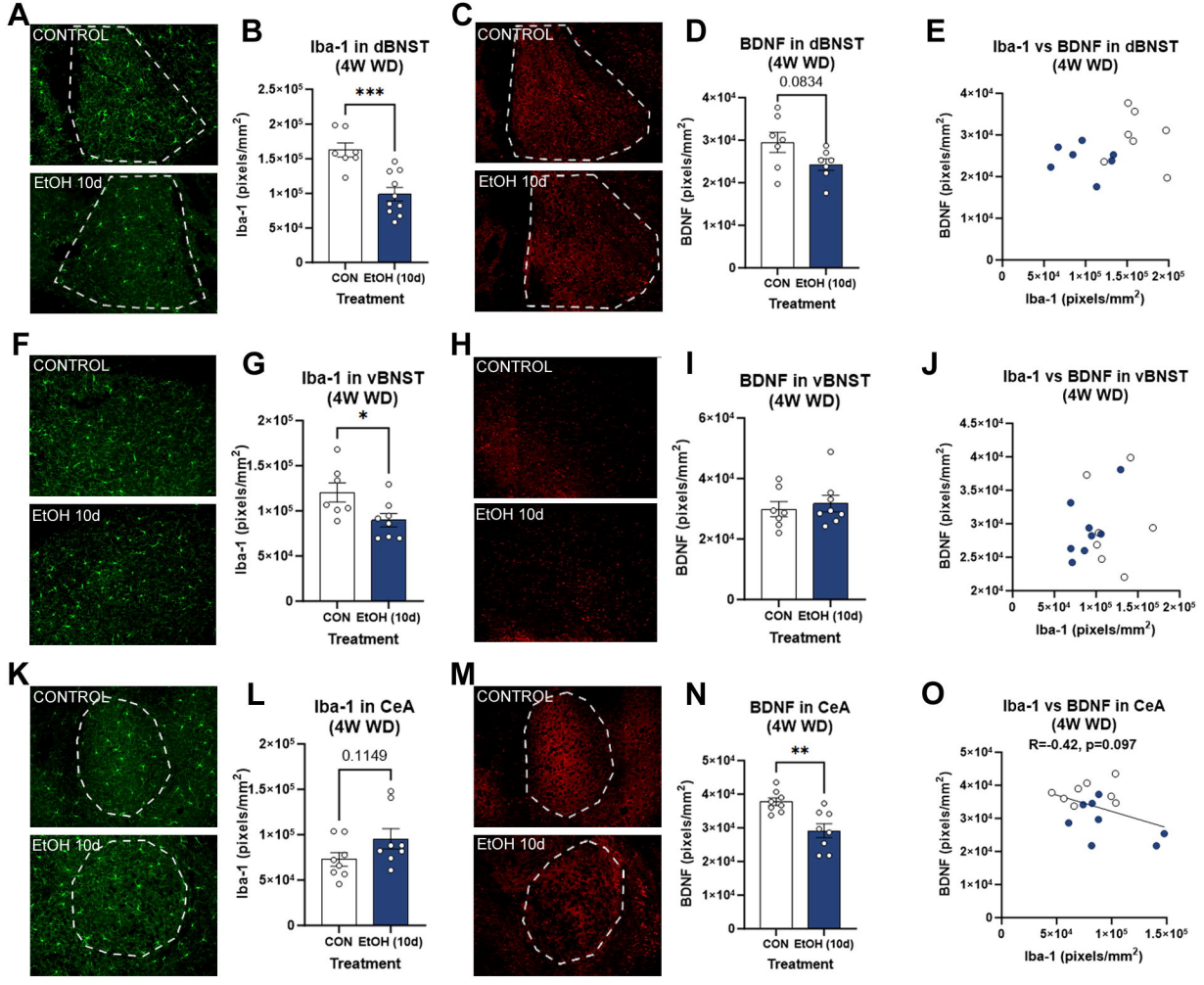
A
CONTROL
EtOH 10d
B
Iba-1 in dBNST
(4W WD)
***
Iba-1 (pixels/mm2)
CON
EtOH (10d)
Treatment
C
CONTROL
EtOH 10d
D
BDNF in dBNST
(4W WD)
0.0834
BDNF (pixels/mm2)
CON
EtOH (10d)
Treatment
E
Iba-1 vs BDNF in dBNST
(4W WD)
BDNF (pixels/mm2)
Iba-1 (pixels/mm2)
F
CONTROL
EtOH 10d
G
Iba-1 in vBNST
(4W WD)
*
Iba-1 (pixels/mm2)
CON
EtOH (10d)
Treatment
H
CONTROL
EtOH 10d
I
BDNF in vBNST
(4W WD)
BDNF (pixels/mm2)
CON
EtOH (10d)
Treatment
J
Iba-1 vs BDNF in vBNST
(4W WD)
BDNF (pixels/mm2)
Iba-1 (pixels/mm2)
K
CONTROL
EtOH 10d
L
Iba-1 in CeA
(4W WD)
0.1149
Iba-1 (pixels/mm2)
CON
EtOH (10d)
Treatment
M
CONTROL
EtOH 10d
N
BDNF in CeA
(4W WD)
**
BDNF (pixels/mm2)
CON
EtOH (10d)
Treatment
O
Iba-1 vs BDNF in CeA
(4W WD)
R=-0.42, p=0.097
BDNF (pixels/mm2)
Iba-1 (pixels/mm2)